Cellular Signalling 64 (2019) 109418

Contents lists available at ScienceDirect

Cellular Signalling

journal homepage: www.elsevier.com/locate/cellsig

Receptor-specific regulation of atrial GIRK channel activity by different Ca^{2+}-dependent PKC isoforms

Anne Niemeyer, Andreas Rinne, Marie-Cecile Kienitz*

Department of Physiology, Ruhr University Bochum, Universitätsstrasse 150, D-44780 Bochum, Germany

ARTICLE INFO

Keywords:
GIRK channel
Receptor desensitization
FRET
PKC
Alpha-adrenergic α_{1B}-receptor
Endothelin receptor

ABSTRACT

G Protein-activated K^+ channels (GIRK) channels are inhibited by depletion of PtdIns(4,5)P_2(PIP_2), and/or channel phosphorylation by proteinkinase C (PKC). By using FRET-based biosensors, expressed in HEK293 cells or in atrial myocytes, we quantified receptor-specific G_q-coupled receptor (G_qPCR) signalling on the level of phospholipase C (PLC) activation by monitoring PIP_2-depletion and diacylglycerol (DAG) formation. Simultaneous voltage-clamp experiments on GIRK channel activity were performed as a functional readout for G_q-coupled α_{1B}- and ET-receptor-induced signalling. G_qPCR-induced fast inhibition of GIRK channel activity is mediated by depletion of PIP_2, whereas phosphorylation of GIRK channels results in delayed, but effective GIRK current inhibition.

We demonstrate a receptor-induced inhibitory component on GIRK activity that is independent of PIP_2-depletion, but attributed to the activation of Ca^{2+}-dependent PKC isoforms. As a novel finding, we demonstrate receptor-dependent differences in GIRK inhibition according to receptor-specific activation of the Ca^{2+}-dependent PKC isoforms PKCα and PKCβ. Pharmacological inhibition of PKCα, but not of PKCβ, abolishes GIRK inhibition induced by stimulation of α_{1B}-receptors. In contrast, ET-R-induced reduction of GIRK activity is sensitive to pharmacological block of PKCβ, but not of PKCα. Coexpression of α_{1B}-receptors (or ET_B-R) and PKCα (or PKCβ) in HEK 293 cells increased homologous receptor desensitization as indicated by a rapid decline of the CKAR FRET signal monitoring receptor activity. These data suggest that receptor-species dependent differences in PKC isoform activation regulate both GIRK channel activity and the strength of the receptor signal via a negative feedback mechanism.

1. Introduction

Parasympathetic control of heart rate and cardiac excitability comprises activation of G protein-activated inwardly rectifying K^+ (GIRK) channels, mainly expressed in the supraventricular tissue. Cardiac GIRK channels are activated by direct interaction of their GIRK1/GIRK4 subunits with βγ subunits of heterotrimeric G proteins upon agonist activation of appropriate $G_{i/o}$-coupled receptors, e.g. following stimulation of M_2 muscarinic receptors by acetylcholine (ACh) or purinergic A_1-receptors by adenosine [1,2]. GIRK channel activity is modulated by diverse signalling pathways downstream of G_s- [3] and G_q-activation [4–9] resulting in either facilitation or inhibition of GIRK currents. Acute and fast inhibition of GIRK channels by stimulation of G_q-coupled receptors (G_qPCRs) is mediated by the phospholipase C (PLC)-catalyzed depletion of PtdIns(4,5)P_2 (PIP_2), which represents an important cofactor for GIRK activation by $G_{\beta\gamma}$ [2,7,10–12].

Furthermore, PLC activation results in IP_3-mediated Ca^{2+} release from internal stores and activation of multiple protein kinase C (PKC) isoforms by the synergistic interaction of Ca^{2+} and diacylglycerol (DAG). Subsequent phosphorylation of GIRK channels results in delayed, but robust inhibition of GIRK currents [10,13,14], probably by reducing the PIP_2-affinity of GIRK channels [10,15,16].

The canonical signalling pathway of activated $G\alpha_q$ subunits comprises hydrolysis of PIP_2 and activation of PKC [17], both acting in concert to inhibit GIRK channels. However, activation of different endogenous G_q-coupled receptors in atrial myocytes induced receptor-specific inhibition of GIRK currents with distinct efficacies and kinetics of inhibition among the different agonists [2]. Thus the question arises, whether receptor-dependent activation of signalling pathways downstream G_q contributes to receptor-specific modulation of GIRK activity.

Up to now, only few studies investigated receptor-specific modulation of GIRK currents in terms of specific PKC isoform activation and/or spatiotemporal dynamics of PIP_2-depletion.

In recent studies, receptor-specific differences in the extent of atrial

* Corresponding author.
E-mail address: cecile.kienitz@rub.de (M.-C. Kienitz).

https://doi.org/10.1016/j.cellsig.2019.109418
Received 9 July 2019; Received in revised form 11 September 2019; Accepted 11 September 2019
Available online 13 September 2019
0898-6568/

GIRK inhibition have been attributed to several factors that determine the strength of PIP_2-depletion during G_qPCR stimulation and the interaction of PIP_2 with its molecular target [7,9,18]. These factors include receptor-dependent changes in the PIP_2 concentration, restricted mobility of PIP_2 and compartmentalization of receptors and signalling components downstream of G_q in microdomains.

Although other studies proposed that a sizable fraction of GIRK current inhibition does not directly reflect PIP_2-depletion, but might be rather attributed to activation of PKC [4,11,13], little is known about the recruitment of different PKC isoforms during receptor-stimulation and their contribution to GIRK inhibition.

Receptor-dependent activation of PKC isoforms and subsequent GIRK inhibition have been investigated in stably Kir3.1/3.2-transfected HEK293 cells, demonstrating that activation of muscarinic M_1 or M_3 receptors specifically activated a Ca^{2+}-independent PKC isoform, in particular PKCδ [19,20]. Stimulation of α-adrenergic receptors in neonatal rat atrial myocytes recruited (not further identified) Ca^{2+}-dependent PKC isoforms to the cell membrane, resulting in pronounced inhibition of acetylcholine (ACh)-activated currents [21]. These divergent results illustrate that the activation of a specific PKC isoform and its contribution to GIRK channel modulation critically depends on the cell type, the molecular composition of GIRK channels and the G_qPCR species.

The fact that multiple factors determine the spatial and temporal specifity of isotype PKC activation (e.g. the cell type [22], the species of G_q-coupled receptors [23,24] the kinetics of membrane translocation [25] or of lipid binding to the membrane-targeting PKC domains [26] and PKC scaffolding in microdomains [27]), might explain why functional studies that address receptor-specific PKC signalling and their regulation of GIRK activity in atrial cells are rare.

To obtain information about the PKC isotype interfering with GIRK channel activity in the native environment of adult rat atrial myocytes, we investigated receptor-specific activation of different PKC isoforms during stimulation of distinct endogenous G_qPCRs. Potential candidates to analyze divergent signalling pathways downstream of G_q activation are α-adrenergic and endothelin (ET)-receptors that induce strong inhibition of GIRK currents in atrial myocytes [2,5].

In the present study, by using a FRET-based biosensor that monitors signalling events downstream of G_q activation and simultaneous whole-cell recordings of GIRK currents, we identified a receptor-induced inhibitory component on GIRK activity that is independent of PIP_2-depletion, but is attributed to PKC activation.

By using selective pharmacological inhibitors of different PKC isoforms, we assigned receptor-dependent differences in GIRK inhibition to receptor-specific activation of the Ca^{2+}-dependent PKC isoforms PKCα and PKCβ.

Furthermore, we point out that receptor-specific activation of a PKC isoform increases homologous desensitization of α-adrenergic and endothelin (ET)-receptors, thus shaping the spatiotemporal activation pattern of G_q signalling components. As a novel finding, we provide evidence that each receptor species was able to recruit a specific PKC isoform. Dependent on this isoform, we observed differences in GIRK channel regulation, suggesting receptor subtype specific negative feedback mechanisms to shape individual GIRK channel responses.

2. Material and methods

2.1. Ethical approval

Rats were killed following protocols in accordance with the guidelines of the European Community (86/609/EEC) and approved by the animal welfare officer of the Ruhr-University Bochum.

2.2. Molecular biology and cell culture

Experiments were performed in HEK 293 cells or in cultured rat atrial myocytes. HEK 293 cells were grown in DMEM medium, supplemented with glutamine (1%) and fetal calf serum (10%) and cultured with penicillin/streptomycin using standard cell culture conditions on 35 mm × 10 mm dishes (Falcon, Corning Inc., Durham, NC, USA). All cell culture media and supplements were purchased from Gibco.

HEK 293 cells were transfected using either polyethyleneimine (PEI) or Lipofectamine (Invitrogen) according to the manufacturer's instructions. Prior to experiments, cells were seeded on sterile, poly-L-lysine-coated glass cover slips and analyzed 48 h after transfections. HEK 293 cells were transiently transfected with cDNAs encoding for GPCRs and the following FRET-biosensors (amount in µg per 35 mm culture-dish): to express α_{1B}-AR or endothelin receptor type B in HEK293 cells: pCDNA3.1$^+$[ADRA1B] (1 µg) or pCDNA3.1$^+$[EDNRB] (1 µg) obtained from the cDNA Resource Center, Bloomsberg, PA, USA.

To monitor the production of the second messenger diacylglycerol (DAG): receptor species as indicated (1 µg) and the biosensor DAGR (0.5), which reports conformational changes of a CFP/YFP-labelled DAG-binding domain of protein kinase C (PKCβ2) [28]. DAGR was kindly provided by Dr. Alexandra Newton (Addgene plasmid # 14865, RRID:Addgene_14,865).

To monitor the breakdown of PIP_2 as an assay for phospholipase C (PLC) activation: receptor species as indicated (1 µg) and a PIP_2 biosensor (0.75) that is based on CFP- and YFP-labelled PH domains of PLCδ1 [11]. In some experiments, cells were infected with Ad-Ci-VSP-T2A-EYFP-PH-PLCδ1-P2A-ECFP-PH-PLCδ1 to express the fluorescence-labelled PH-domains and the voltage-sensitive phosphoinositide phosphatase Ci-VSP simultaneously [11,29]. The tricistronic virus encoding for Ci-VSP and the two PH-domains will be termed Ad-PIP_2-tool.

To monitor the increase in $[Ca^{2+}]_i$: receptor species as indicated (1 µg) and the Twitch-2B biosensor (0.25 µg) that has a calcium binding motif based on the C-terminal domain of *Opsanus tau* TnC [30]. Twitch-2B pcDNA3 was kindly provided by Dr. Oliver Griesbeck (Addgene plasmid #49531, RRID:Addgene_49,531).

To monitor PKC activity: receptor species as indicated (1 µg) and the CKAR biosensor (1 µg) [28] that contains a PKC substrate sequence flanked by a flexible linker sequence. CKAR was a gift from Dr. Alexandra Newton (Addgene plasmid # 14860, RRID:Addgene_14,860).

For some experiments cells were co-transfected with 0.5 µg of a plasmid encoding for wild type PKCα (WT-PKCα) or wild-type PKCβ1 (WT-PKCβ1) [31], kindly provided by Dr. Bernard Weinstein via Addgene (WT-PKCα # 21232 RRID:Addgene_21,232, WT-PKCβ1 # Plasmid #16378, RRID:Addgene_16,378).

2.3. Fluorescence microscopy and imaging

All experiments were performed using single cells at ambient temperature. Fluorescence was recorded using an inverted microscope (Zeiss Axiovert 200, Carl Zeiss AG, Göttingen, Germany) equipped with a Zeiss oil immersion objective (100 × /1.4), a Polychrome V illumination source and a photodiode-based dual emission photometry system suitable for CFP/YFP-FRET (FEI Munich GmbH, Germany). For FRET measurements, single cells were excited at 435 nm wavelength with light pulses of variable duration (10 ms to 50 ms; frequency: 5 Hz) to minimize photobleaching. Corresponding emitted fluorescence from CFP (F_{480} or F_{CFP}) or from YFP (F_{535} or F_{YFP}) was acquired simultaneously and FRET was defined as ratio F_{YFP}/F_{CFP}. Fluorescent signals were recorded and digitized using a commercial hardware/software package (EPC10 amplifier with an integrated D/A board and Patchmaster software, HEKA, HEKA Elektronik, Germany). Details on optical filters and beam splitters of the setup are given in [11]. The individual FRET were normalized to the initial ratio value before agonist application ($FRET/FRET_0$).

2.4. Isolation and culture of atrial myocytes

Rats were killed with the following protocol in accordance with the guidelines of the European Community (86/609/EEC) and approved by the animal welfare officer of the Ruhr-University Bochum. WKY rats of either sex (weight around 200 g) were anesthesized by intravenous injection of urethane (1 g/kg). The chest was opened, the heart was removed and mounted on the cannula of a Langendorff perfusion system for coronary perfusion at constant flow. Isolated hearts were perfused with a nominally Ca^{2+}-free solution (mmol/L) (NaCl 140, KCl 5.4, $MgCl_2$ 1, HEPES 10, *N*-acetyl-cysteine 3, pyruvic acid 5, EGTA 1.25, pH 7.4) for 10 min, then with enzyme solution (mmol/L) (NaCl 140, KCl 5.4, $MgCl_2$ 1, HEPES 10, collagenase II (Worthington Biochemical Corporation, NJ, USA) (1 mg/mL), protease type XIV (Sigma Aldrich, München) (0.25 mg/mL), DNAse I (Sigma) (0.1 mg/mL), taurine (Sigma) (0.625 mg/mL), 2,3-Butanedione monoxime (Sigma) (0.5 mg/mL) for 15 min. Hearts were removed from the cannula, ventricles were cut off and atria were mechanically dissected with fine forceps and chopped into 1 mm^3 chunks.

To isolate single cells, atrial tissue chunks were agitated using a Pasteur pipette in enzyme solution for 30 min. Enzymatic activity was disrupted by adding nominally Ca^{2+}-free solution supplemented with fatty acid free albumine (Sigma) (1 mg/mL) and taurine (1.25 mg/mL). To avoid contracture of atrial myocytes during reintroduction of external Ca^{2+}, $[Ca^{2+}]_o$ in the supernatant solution was stepwise increased to 2 mmol/L within 2 h by exchanging the supernatant solution with a solution (mmol/L) (NaCl 140, KCl 5.4, $MgCl_2$ 1, HEPES 10, pH 7.4) supplemented with 0.5 mmol/L, 1 mmol/L, 1.5 mmol/L and 2 mmol/L $CaCl_2$.

Cells were plated at a low density (several hundred cells per 35 mm dish) and cultured in FCS-free medium (HEPES-buffered M199, PAA Laboratories, Pösching, Austria) supplemented with ITS (insulin/transferrin/selenium), Gentamycin (1.4 µg/mL, Sigma Aldrich, München) and Kanamycin (0.7 µg/mL, Sigma Aldrich). To express Ad-Ci-VSP-T2A-EYFP-PH-PLCδ1-P2A-ECFP-PH-PLCδ1 (termed Ad-PIP_2-tool, [11]) cardiac cells were infected with Ad-PIP_2-tool one day after isolation and analyzed 48 h after infection. MOIs were adjusted to reach an infection rate of 50% (assessed as EYFP-positive cells). Non-infected myocytes were used experimentally from day 1 until day 6 after isolation.

2.5. Solutions and chemicals

For FRET measurements an extracellular solution of the following composition was used (mmol/L): NaCl 122, KCl 5.4, $CaCl_2$ 0.5, $MgCl_2$ 1.0, Hepes/NaOH 10.0, pH 7.4. For whole cell measurements of membrane currents an extracellular solution of the following composition was used (in mmol/L): NaCl 122, KCl 20, $CaCl_2$ 0.5 or concentration as indicated, $MgCl_2$ 1.0, HEPES/NaOH 10.0 (pH 7.4). The pipette solution contained (in mmol/L): K-aspartate 100, KCl 40, NaCl 5.0, $MgCl_2$ 2.0, Na_2ATP 5.0, EGTA 2.0, GTP 0.025, and HEPES/KOH 20.0 (pH 7.4) indicated as "GTP"-pipette solution. In some experiments, EGTA was substituted by BAPTA 5.0 mmol/L (termed as "GTP + BAPTA"). The K^+ reversal potential under this condition was calculated as −48 mV. In some experiments, 0.5 mmol/L of the non-hydrolyzable GTP-analog GTPγ-S was included in the pipette solution. Standard chemicals were from Merck (Darmstadt, Germany). EGTA, HEPES, Guanosine 5′-triphosphate sodium salt hydrate (GTP), Guanosine 5′-(γ-thio)-triphosphate tetralithium salt (GTPγ-S), Na_2ATP, Acetylcholine-chloride (ACh), chelerythrine chloride and phenylephrine were from Sigma-Aldrich (Taufkirchen, Germany). Endothelin-1, Gö6976 and Ro32–0432 were obtained from Biomol, Hamburg, Germany. Enzastaurin was from Bio-Techne, Wiesbaden, Germany.

2.6. Current measurement

Membrane currents were measured using whole-cell patch clamp. Pipettes were fabricated from borosilicate glass and were filled with the solution listed above (direct current resistance, 4–6 MΩ). Currents were measured by means of a patch clamp amplifier (List LM/EPC 7, Darmstadt, Germany). Atrial cells were voltage-clamped at a holding potential of −90 mV, i.e. negative to the equilibrium potential for K^+ (E_K = −48 mV), resulting in inward K^+ currents. Every 10 s, voltage ramps (duration 500 ms) from −120 mV to +60 mV were applied to assess stability of the recording conditions and to generate I/V curves (membrane currents in response to depolarizing voltage ramps are shown as upward deflections).

Signals were filtered (corner frequency, 1 kHz), digitally sampled at 1 kHz and stored on a computer equipped with a hardware/software package (ISO2, MFK, Niedernhausen, Germany) for voltage control, data acquisition and data analysis. Experiments were performed at ambient temperature (23–26°C). Rapid exposure to solutions containing agonists or inhibitors was performed by means of a custom-made solenoid-operated flow system permitting a change of solution around an individual cell with a half time of about 100 ms. For measurements cells devoid of contact with neighboring cells were selected.

2.7. Statistical analysis

Statistical analysis was performed with the software OriginPro2018b (OriginLab Corporation, Northampton, MA, USA, RRID:SCR_014212). All data are presented as individual observations or summarized data (mean ± S.E. of n cells). Student's *t*-Test was used to compare the means between two groups if the data passed the Shapiro-Wilk normality test and the equal variance test (Levene). P-values < 0.05 were considered statistically significant. If the data were not distributed normally, the Mann-Whitney Rank Sum test was used. Comparisons between multiple groups were performed using One-Way ANOVA after testing normal distribution and equal variance. The Holm-Sidak post-hoc test was assessed for statistical significance ($p < 0.05$). In case that the assumption of homogeneity of variance between the groups was violated in the ANOVA analysis, Kruskal-Wallis-Anova and Dunn post hoc test were used. P-values < 0.05 were considered statistically significant. In general, p-values < 0.05 were marked by an asterisk, p-values < 0.01 were marked by two asterisks and p-values < 0.001 were marked by three asterisks. To compare peak values of G_qPCR-induced FRET signals, peak data were measured within a frame of 5 s (corresponding 25 data points) or 10 s (50 data points) and tested for statistical significance by Student's *t*-Test or Mann-Whitney Rank Sum test.

3. Results

3.1. Inhibition of atrial GIRK currents by various G_qPCR agonists

To investigate the inhibitory effect of α-adrenergic and ET-receptor stimulation on rat atrial $IK_{(ACh)}$, we used a double pulse protocol established in a previous study on mouse atrial myocytes [2] with paired application of acetylcholine in the presence and absence of specific G_qPCR agonists.

In rat atrial myoyctes, brief application of a saturating concentration of acetylcholine (10 µmol/L) induced a rapidly activating transient inward current followed by acute desensitization (Fig. 1A). Characteristics of this $IK_{(ACh)}$ have been analyzed in detail previously, respectively the rapid current decay after peak $IK_{(ACh)}$ and the typical strong inward rectification of the background-subtracted current voltage-relation (see also I/V curve in Fig. 2E). Furthermore, the acute current desensitization is instantaneously reversible as soon as current deactivation upon washout of the agonist is complete [32]. In line with these previous findings, the response to a second challenge by ACh was

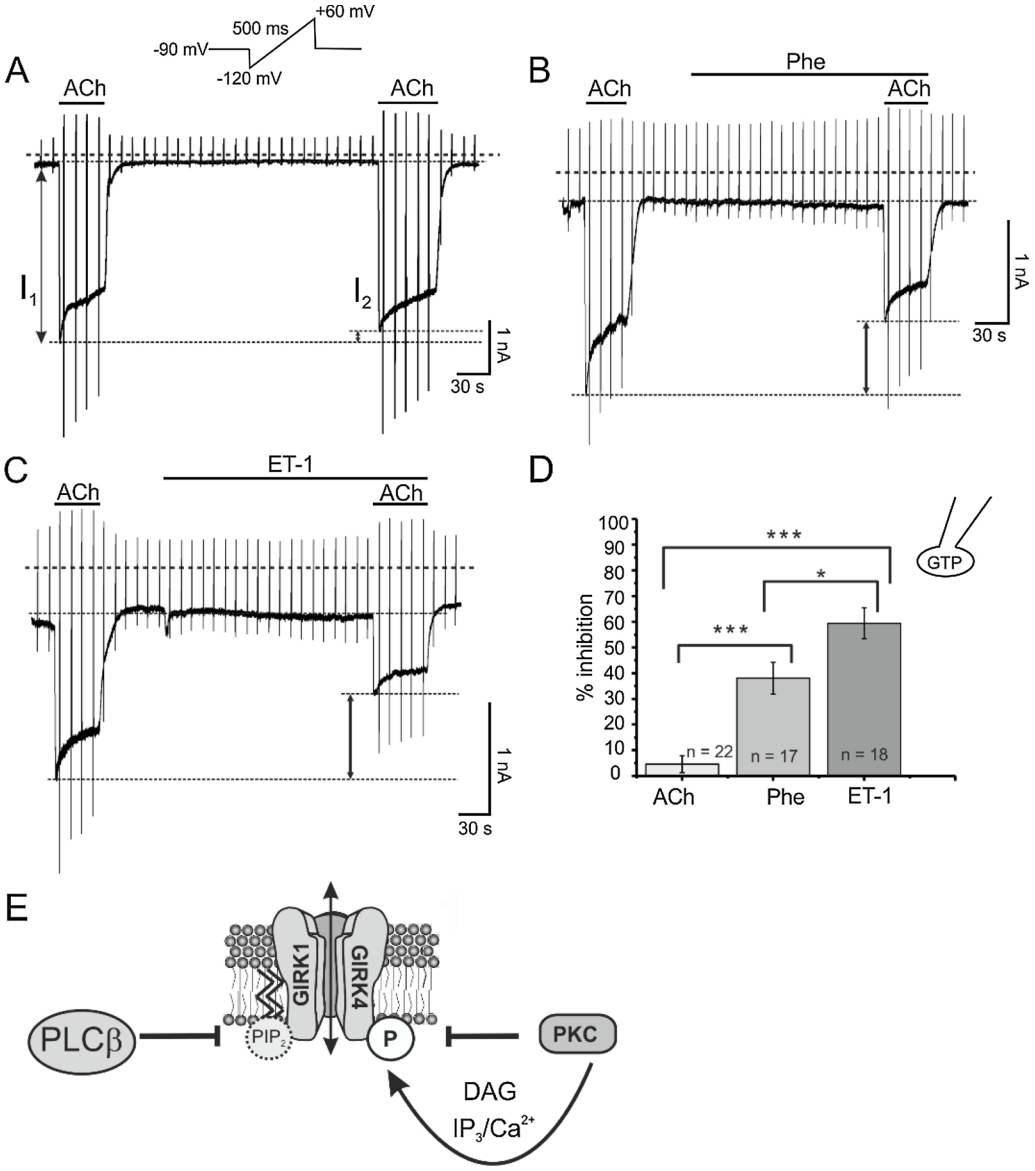

Fig. 1. Inhibition of acetylcholine-activated GIRK currents ($IK_{(ACh)}$) by phenylephrine and endothelin.
Representative current recordings of ACh-activated (10 μmol/L) GIRK currents during paired ACh applications in the presence (B, C) and absence (A) of specific G_qPCR agonists ($[Ca^{2+}]_o$ = 2 mmol/L). The first response to ACh in the absence of G_qPCR agonists (termed I_1) was related to the amplitude of $IK_{(ACh)}$ recorded 3 min after application of phenylephrine (Phe, 100 μmol/L, B) or endothelin (ET-1, 10 nmol/L, C) (termed I_2). Dashed lines indicate zero current level. Inset: Scheme of the experimental protocol. D. Summarized data of GIRK inhibition (mean ± S.E.) as indicated by the reduction of I_2 as compared to I_1. One-way ANOVA was applied for group comparisons and Student's *t*-Test (with Welch correction) was used for pairwise comparisons. P-values < 0.05 were considered statistically significant and marked by one asterisk, p-values < 0.001 by three asterisks. n = number of experiments. n.s. = not significant. E. Schematic illustration of different G_qPCR-induced mechanisms of GIRK channel modulation.

only slightly reduced by 4.6 ± 3.3% (mean ± S.E., n = 22, Fig. 1D).

To estimate the inhibitory potential of different G_qPCR agonists, we probed GIRK inhibition by coapplication of saturating concentrations of phenylephrine (100 μmol/L) or endothelin (10 nmol/L) analogous to a previous study [33]. As a rule, the peak $IK_{(ACh)}$ amplitude at the first response to ACh was set as control (I_1). G_qPCR agonists were applied 3 min before the second application of ACh and the amplitude of this second $IK_{(ACh)}$ in the continuous presence of an agonist (I_2) was related to I_1 to quantify receptor-induced current inhibition.

In the presence of either phenylephrine or endothelin, the amplitude of I_2 was significantly reduced as compared to I_2 in the absence of both G_qPCR agonists (compare Fig. 1A–C) with endothelin being more efficient in inhibiting $IK_{(ACh)}$ (summarized data in Fig. 1D). In principle, the signalling pathway of both α-adrenergic and endothelin ET-receptors results in PLCβ-catalyzed depletion of PIP_2, IP_3-mediated Ca^{2+} release from internal stores and PKC activation by Ca^{2+} and DAG (see cartoon in Fig. 1E). Several mechanisms might account for the receptor-specific efficiency of GIRK inhibition, including activation of different branches of the $G\alpha_q$-signalling pathway, different efficiencies in PIP_2-depletion or receptor-dependent activation of PKC-isoforms.

The data presented in Fig. 1 are in good agreement with an earlier work [2], describing receptor-specific inhibition of adenosine-activated GIRK currents in mouse atrial myocytes. However, since a very early work on $IK_{(ACh)}$ modulation by G_qCPRs postulated a phenylephrine-induced activation of single muscarinic K^+ channels recorded in the cell-attached patch configuration [34], this experimental protocol might underestimate the extent of G_qPCR-induced GIRK inhibition due to superimposition of activating and inhibitory effects on channel activity.

To avoid superimposition of potentially activating and inhibitory effects of G_qPCR agonists, we aimed to investigate G_qPCR effects on pre-activated GIRK currents to isolate the inhibitory effect on $IK_{(ACh)}$. However, activation of $IK_{(ACh)}$ by a long-lasting application of a saturating ACh concentration (10 μmol/L) in the absence of G_qPCR agonists per se resulted in a current decay of about 20% (Fig. 2A and H). This intrinsic current decay might be attributed to current and/or receptor desensitization, but presumably interferes with G_qPCR-induced GIRK current inhibition.

To maintain a stable amplitude of GIRK channel current, myocytes were continuously exposed to ACh and loaded with GTPγ-S (0.5 mmol/L) via the patch pipette. Fig. 2B shows a representative current trace from a native atrial cell to demonstrate the effect of GTPγ-S loading which resulted in maximal and irreversible activation of GIRK channels. Once activated, the current remained fairly constant for several minutes

of recording in the continuous presence of ACh (see also Fig. 2H). At the end of each GTPγ-S experiment, GIRK channels were blocked by 1 mM Ba^{2+} to assess stability of the patch recording.

Analogous to the protocol established in [2] and shown in Fig. 1 of the present study, G_q-activating agonists and ACh were applied simultaneously.

To evaluate if the initial G_i-induced GIRK activation is blunted by simultaneous G_q-induced PIP_2-depletion, we analyzed the current amplitude of the peak $IK_{(ACh)}$ in the presence and absence of G_qPCR agonists, but, as indicated in Fig. 2G, no significant differences in peak

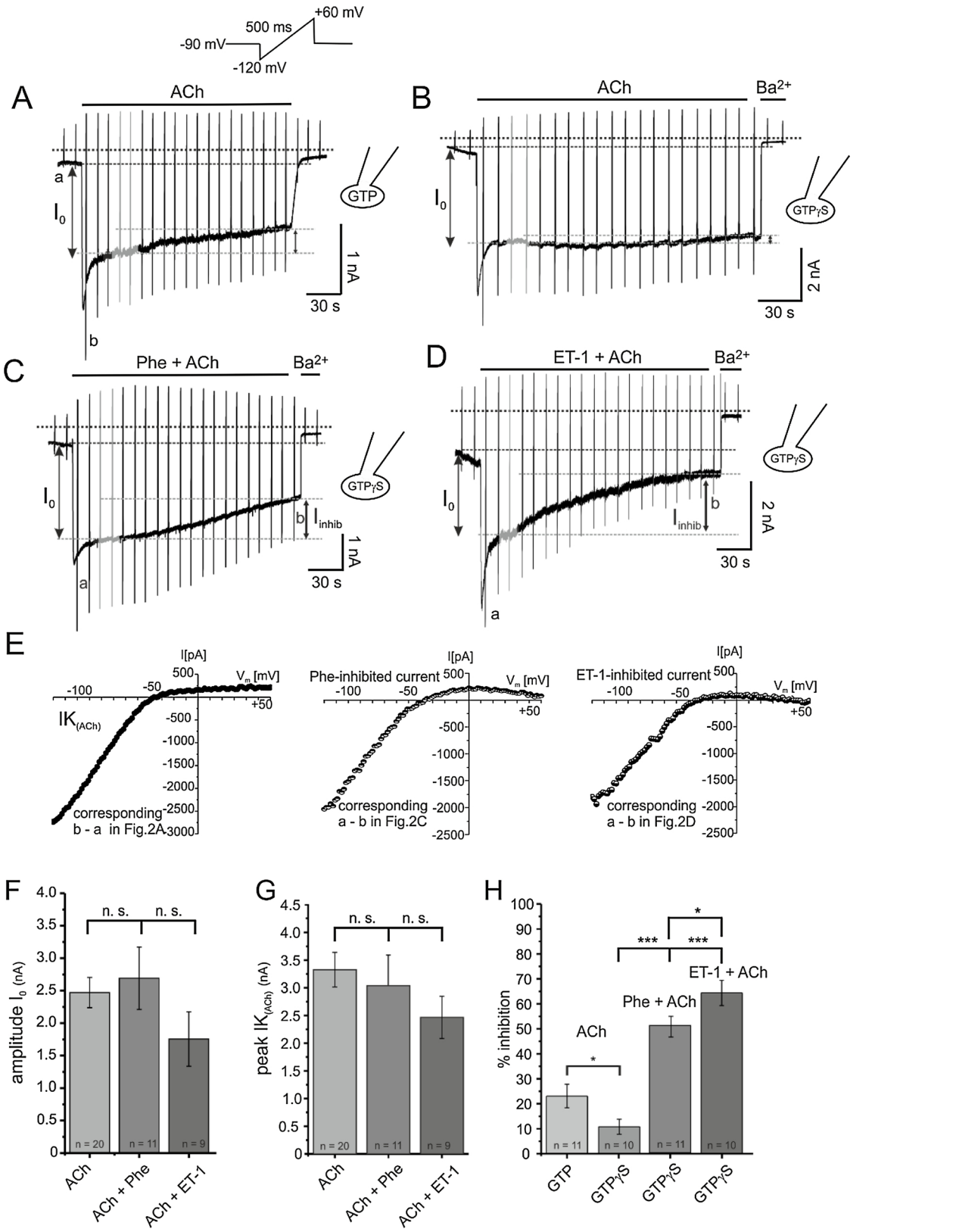

(caption on next page)

Fig. 2. Inhibition of GTPγ-S-activated GIRK currents during stimulation of atrial α_1-adrenergic or ET- receptors.
A. Representative recording of ACh-activated (10 μmol/L) GIRK currents measured with a GTP (25 μmol/L)-containing pipette solution. Inset: Scheme of the experimental protocol. B. Recording of GTPγ-S (0.5 mmol/L)-activated GIRK currents in the continuous presence of ACh. 1 mmol/L Ba^{2+} was applied at the end of the experiment to assess stability of the patch recording. C/D. Representative GTPγ-S-activated GIRK currents during coapplication of ACh and either Phe (100 μmol/L) or ET-1 (10 nmol/L). E. I/V curves of atrial GIRK currents obtained by subtraction of voltage ramp-induced changes of current in the presence and absence of ACh (10^{-5} mol/L) (left panel, corresponding lower case letters b- a in Fig. 2A or of the Phe-inhibited current (middle panel, corresponding a - b in Fig. 2C) or of the ET-1-inhibited current (right panel, corresponding lower case letters a – b in Fig. 2D).
F. Summarized data indicating amplitude of I_0 in the presence and absence of G_qPCR agonists. Steady-state amplitude (I_0) was defined as a period of ≥ 20 s of stable membrane current following peak $IK_{(ACh)}$. Multiple group comparisons were assessed with Kruskal-Wallis ANOVA and Dunn post-hoc test. n.s. = not significant.
G. Summarized data indicating peak $IK_{(ACh)}$ amplitude in the presence and absence of G_qPCR agonists. Multiple group comparisons were assessed with One-way ANOVA and Holm-Sidak post hoc test. n.s = not significant.
H. Summarized data indicating GIRK current decay by various agonists. Current decay was quantified by relating the GIRK amplitude at the end of agonist application (I_{inhib}) to the initial steady-state amplitude of ACh-activated GIRK current (I_0, highlighted in grey) as indicated by the dashed lines and arrows in A – D. Means of data obtained with GTP-containing pipette solution and with GTPγ-S were compared by Student's t-Test, multiple group comparison were performed by One-way ANOVA and Holm-Sidak test. P-values < 0.05 were considered statistically significant and marked by an asterisk, p-values < 0.001 were marked by three asterisks. Number (n) of experiments is indicated throughout. n.s = not significant.

$IK_{(ACh)}$ were observed. However, coapplication of ACh and either Phe or ET-1 resulted in a gradual inhibition of the pre-activated current to a stable steady-state level (Fig. 2C,D), suggesting slower kinetics of GIRK inhibition by G_q-induced signalling pathways than G_i-induced GIRK activation. The current voltage-relations of the agonist-inhibited current components were characterized by the typical strong inward rectification of GIRK currents, i.e. a massive reduction in slope conductance at voltages positive to the equilibrium potential for K^+ (compare I/V curves in Fig. 2E), indicating that G_qPCR activation inhibits GIRK channels itself rather than modulating other ion currents.

To quantify the extent of GIRK inhibition, we determined the quasi-steady state amplitude (I_0) that followed the rapid decay of peak $IK_{(ACh)}$ and remained stable for at least 20 s and related the G_qPCR-induced current reduction (I_{inhib}) to this initial value. To evaluate if the amplitude of I_0 was reduced by a slowly developing G_q-induced PIP_2-depletion, we determined I_0 in the presence and absence of G_qPCR agonists. However, as shown in Fig. 2F, no significant differences were detected.

In GTPγ-S-dialyzed atrial myocytes, 100 μmol/L phenylephrine (Phe) and 10 nmol/L ET-1 caused an inhibition of $IK_{(ACh)}$ of about 52% and 64% (see summarized data in Fig. 2H) compared to 38% for α_{1B}-AR- and 59% for ET-1-induced inhibition in the absence of GTPγ-S (see Fig. 1D). The strong Phe- and ET-1- induced GIRK inhibition in the presence of GTPγ-S is attributed to the persistent activation of G_q proteins that results in long-lasting PLC activation with pronounced PIP_2-depletion and PKC activation. Furthermore, the persistent G_q activation simultaneously activates both branches of G_q signalling pathways that act synergistically to inhibit GIRK currents. As a consequence, receptor-specific spatiotemporal differences in PIP_2-depletion or PKC activation are less pronounced in the presence of GTPγ-S.

To evaluate receptor-specific differences in PIP_2-depletion or receptor-dependent activation of PKC-isoforms, we aimed to quantitatively analyze signalling events during α-adrenergic and ET-receptor stimulation by means of FRET-based biosensors that monitor signalling molecules downstream of G_q protein activation. These experiments were performed in the absence of GTPγ-S to allow transient activation of G_q-dependent pathways.

3.2. Analysis of α_{1B}-adrenergic receptor- and ET_B-receptor-induced signalling pathways downstream of G protein activation in HEK 293 cells and in atrial myocytes

To analyze receptor-dependent aspects of signalling downstream of G_q, we analyzed the time-course of DAG formation in HEK cells expressing either α_{1B}-adrenergic receptors (α_{1B}-AR) or ET_B-R and the fluorescent biosensor DAGR which reports formation of DAG by an increase in the FRET ratio [28] (see also scheme in Fig. 3E). The DAGR biosensor has been established as a powerful tool for studying the kinetics of G_q-coupled receptor activity [28,35]. As reported previously, the time course of DAG formation can be used to analyze the rate of homologous receptor desensitization during agonist exposure [35] and to evaluate receptor-specific differences in receptor activity [24].

The representative recordings in Fig. 3C and D show the effects of G_qPCR-stimulation on DAG production during application of phenylephrine or ET-1. Activation of α_{1B}-receptors and ET_B receptors caused a rapid increase in FRET ratio, reflecting activation of PLC and formation of DAG at the plasma membrane, followed by a decrease of DAG formation during receptor stimulation.

The time course of DAG formation is determined by the specific activation of heterologously expressed α_{1B}-receptors and ET_B receptors. In agreement with this notion, application of Phe or ET-1 in the absence of heterologously expressed receptors (-α_{1B}-R/DAGR, -ET_B − /DAGR) did not result in DAG formation, thus excluding background activation of endogenous receptors (Fig. 3A and B). Both the onset (measured as t½, Fig. 3I) and the amplitude of the ET-1-induced DAG signal (see asterisks in Fig. 3D) were significantly different from the Phe-induced DAG signal. The decay of the G_qPCR-induced DAG signal reflects intrinsic receptor properties such as the duration of receptor activity. The summarized data in Fig. 3J, expressed as the ratio $FRET_{30s\ after\ peak}$/$FRET_{peak}$, indicate a 34% reduction of the DAG signal during α_{1B}-AR stimulation. In contrast, during stimulation of ET_B-receptor, we observed only a decline in DAG of about 20%. As recently reported [24], receptor-dependent differences in the time course of DAG reduction reflect receptor-specific differences in homologous receptor desensitization and represent a mechanism of effector modulation, e.g. by controlling the duration of PIP_2-depletion and/or the recruitment of different PKC isoforms.

To investigate whether α_{1B}- and ET_B-specific differences in receptor activity were also evident at the level of PLC activation, we analyzed G_qPCR-induced PIP_2-depletion in HEK cells by utilizing a biosensor that reports the depletion of membrane PIP_2 with a decrease in FRET ratio [11] (see also scheme in Fig. 3H). As illustrated in the summarized FRET recordings in Fig. 3F and G, stimulation of α_{1B}-receptors or ET_B receptors caused a decrease in FRET ratio, indicating membrane PIP_2-depletion. Both α_{1B}-AR- and ET_B-mediated PIP_2-depletion showed a biphasic time course: During agonist application, the FRET signal slowly decreased for about 50 s, followed by a slight decay. The rates of the initial FRET decrease (evaluated by t½, Fig. 3I) were almost identical for both agonists. Furthermore, the summarized $FRET_{30s\ after\ peak}$/$FRET_{peak}$ ratios in Fig. 3J indicate similar rates of the subsequent FRET decay. During activation of α_{1B}-receptors, the PIP_2-FRET signal declined by about 23% as compared to 19% during stimulation of ET_B receptors. Although we found no significant differences in the time course of G_qPCR-induced PIP_2-depletion (Fig. 3I and J), stimulation of ET_B receptors resulted in pronounced PIP_2-depletion as indicated by the larger decrease of the FRET signal as compared to the α_{1B}-AR-induced signal. Statistical analysis of the peak values of G_qPCR-induced PIP_2-depletion indicated that ET-1-induced PIP_2-depletion was significantly different from Phe-induced FRET signals (marked by asterisks in

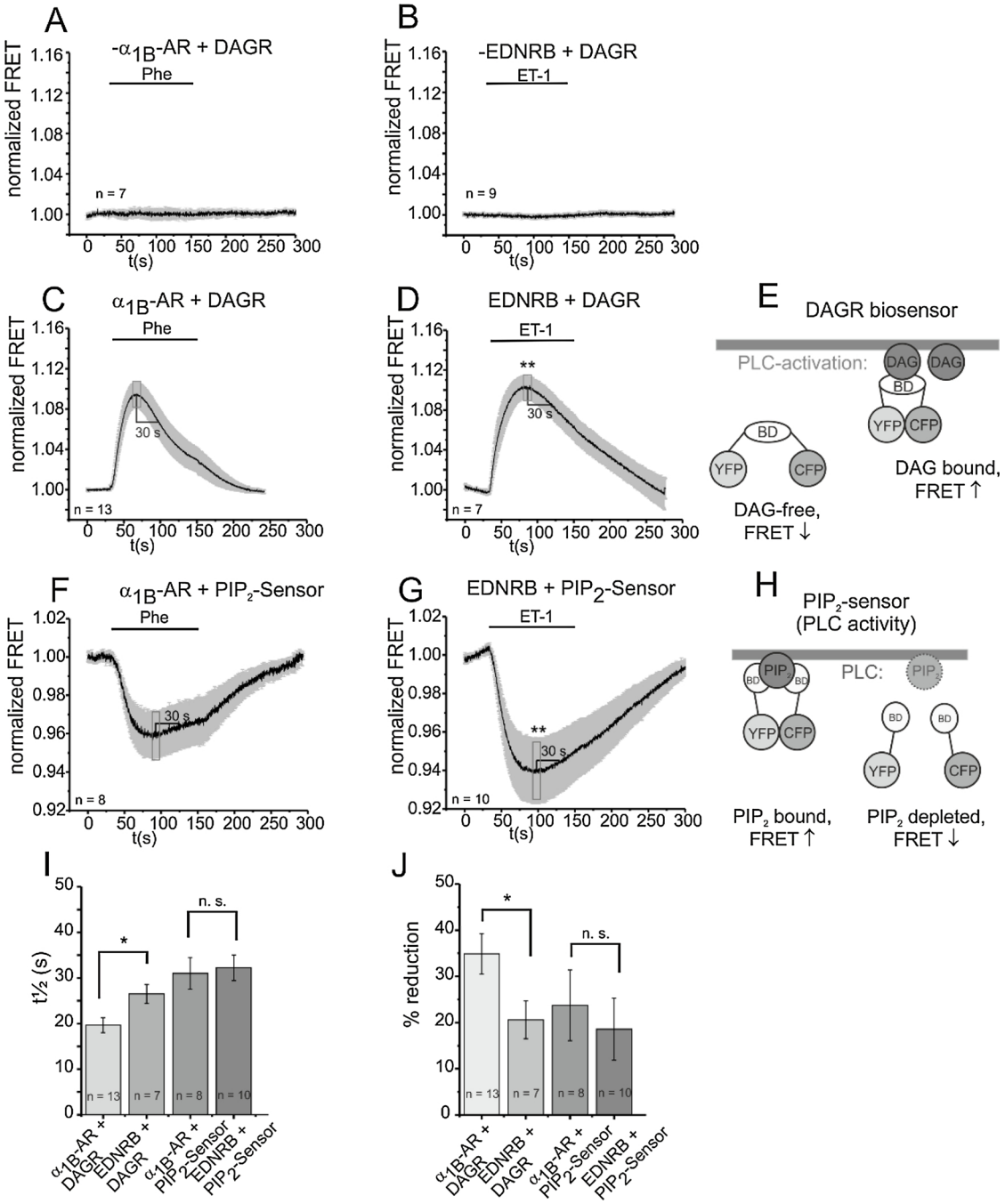

Fig. 3. Activation of signalling pathways downstream G_q by α_{1B}-receptor and ET_B-receptors in HEK 293 cells.

Summarized FRET-recordings (mean ± S.E.) from -α_{1B}-receptor/DAGR- (A), +α_{1B}-receptor/DAGR- (C), -ET_B-receptor/DAGR- (B) or + ET_B-receptor/DAGR- (D) expressing HEK 293 cells, monitoring DAG formation during application of 10 μmol/L Phe or 100 nmol/L ET-1 (0.5 mmol/L $[Ca^{2+}]_o$ was present throughout). Student's t-Test was used to compare peak values of Phe-and ET-1-induced DAG signals (peak data were measured within a frame of 10 s as indicated by grey boxes, corresponding 50 data points). $P < 0.01$ was indicated by the asterisks in D.

E: Scheme of a FRET biosensor for DAG production. Activation of PLC results in DAG formation and translocation of the DAG binding domains to the plasma membrane, resulting in an increase of the FRET ratio.

F.G. Summarized FRET-recordings from α_{1B}-receptor/PIP_2-biosensor- (F) or ET_B-receptor/ PIP_2-biosensor- (G) expressing HEK 293 cells, monitoring PLC activation during application (duration 120 s) of 10 μmol/L Phe or 100 nmol/L ET-1. For comparing the amplitudes of Phe- and ET-1 induced PIP_2-depletion, peak data were measured within a frame of 10 s as indicated by the grey boxes (corresponding 50 data points) and evaluated by the Mann-Whitney Rank Sum test. $P < 0.01$ was indicated by the asterisks in G.

H. Scheme of a FRET biosensor monitoring the activation of PLC and subsequent PIP_2-depletion. Hydrolysis of PIP_2 causes translocation of the fluorescent protein-tagged PIP_2 binding domains (pleckstrin homology domains) from the membrane, resulting in a decrease of the FRET ratio.

I. Summarized data evaluating the rates of DAG formation and PIP_2-depletion (half times, t½). Significance was tested with Student's *t*-Test. P-value < 0.05 was considered statistically significant and marked by an asterisk. n.s. not significant.

J. Summarized data of the decay of DAG formation or decline of PIP_2 reduction during agonist application (determined by the ratio $FRET_{30s\ after\ peak}/FRET_{peak}$). Student's t-Test was used for comparing α_{1B}-DAGR and EDNRB-DAGR, Mann-Whitney Rank Sum test for comparing α_{1B}-PIP_2 and EDNRB-PIP_2. P-value < 0.05 was considered statistically significant and marked by an asterisk. Number (n) of experiments is indicated throughout.

Fig. 3G).

It is tempting to speculate that the different amplitudes of Phe- and ET-1-induced FRET signals are attributed to the prolonged activity of ET_B-receptors as compared to the activity of α_{1B}-receptors. Alternatively, discrepancies in the number of activated α_{1B}- and ET_B-receptors or differences in receptor expression levels might account for the different extent of G_qPCR-induced DAG formation and PIP_2-depletion. Thus, evaluating the amplitude of FRET signals might be insufficient to assess receptor-specific differences in downstream G_q signalling. However, as recently described [24], the time course of FRET responses is rather independent of receptor expression levels and reflects intrinsic receptor properties such as the rate of desensitization during agonist exposure. In line with these findings, the different time courses of DAG decay during stimulation of α_{1B}- and ET_B-receptors (Fig. 3J) indicate receptor-specific differences in receptor activity that might result in different kinetics of G_q signalling and receptor-dependent modulation of effectors.

To evaluate if receptor-dependent differences in receptor activity determine the extent of α_{1B}- and ET-receptor-induced PIP_2-depletion in the native environment of atrial cells, we monitored G_qPCR-induced dynamic changes in membrane PIP_2 by means of a FRET biosensor. To correlate the time course of PIP_2-depletion to GIRK inhibition, we performed simultaneous patch-clamp experiments to monitor GIRK activity and FRET recordings in atrial myocytes coexpressing the voltage-sensitive phosphatase Ci-VSP and the PIP_2 biosensor (termed Ad-PIP_2-tool, see scheme in Fig. 4F). The voltage-sensitive phosphoinositide phosphatase Ci-VSP, originally cloned from *Ciona intestinalis* [29], consists of a voltage sensor domain with homology to subunits of voltage-activated K^+ (Kv) channels and a phosphatase domain sharing homology to the phospholipid-phosphatase PTEN that dephosphorylates PI(3,4,5)P_3 and PI(4,5)P_2 [29,36]. The phosphatase activity of Ci-VSP can be switched on and off in a graded manner by depolarization/repolarization, resulting in rapid and reversible changes in membrane PIP_2 without activating PLC-mediated downstream signalling pathways. By infecting atrial myocytes with the Ad-PIP_2-tool (an adenovirus based on a tricistronic shuttle vector containing the cDNAs for Ci-VSP and two fluorescent PH-domains (ECFP-PH-PLCδ1 and EYFP-PH-PLCδ1 [11]), changes in membrane PIP_2 induced by activation of Ci-VSP and by stimulation of G_qPCRs can be monitored simultaneously.

Fig. 4A compares ACh-activated GIRK current traces from a native myocyte (left trace) and a myocyte infected with the Ad-PIP_2-tool (right trace), reflecting the change in membrane current caused by a step depolarization from the holding potential of −90 mV to +60 mV (4 s). This depolarization resulted in an instantaneous outward current that rapidly declined due to the block by intracellular polyamines and Mg^{2+}. Upon repolarization, the baseline current level was reached quasi instantaneously in native cells, due to the rapid kinetics of the Mg^{2+}/polyamine unblock. In Ad-PIP_2-tool-infected myocytes, Ci-VSP-induced PIP_2-depletion resulted in a strong reduction of the inward current (see arrow), which slowly recovered (see dashed lines).

Simultaneous changes in PIP_2 levels (indicated as the FRET ratio of the PIP_2 biosensor) and corresponding changes in GTPγ-S-activated GIRK currents during a step depolarization from −90 mV to +60 mV (4 s) are traced in Fig. 4B to illustrate that the time courses of PIP_2 depletion/resynthesis matched the inhibition and recovery of GIRK currents (labelled “a” in both traces). Further details on the kinetics of modulating cardiac GIRK channel activity by PIP_2-depletion/replenishment have been analyzed in detail in a previous study [11].

Fig. 4C and D show representative experiments in which effects of Ci-VSP-activation and activation of endogenous α_1-AR or endothelin receptors on GIRK activity and PIP_2-depletion were compared. Analogous to Fig. 4B, the Ci-VSP-induced signals reflecting instantaneous GIRK current inhibition matched the changes in FRET ratio. Application of Phe (100 μmol/L, C) or ET-1 (10 nmol/L, D) caused an additional decrease in the FRET ratio paralleled by further inhibition of the GTPγ-S activated GIRK current. Although the onset of PIP_2 depletion might display slight cell-to-cell variations, the time course of the initial FRET decrease was not significantly different between Phe- and ET-1-induced PIP_2-depletion (Phe: $t½ = 83.1 \pm 7.6$ s, n = 12; ET-1: $t½ = 88.7 \pm 8.2$ s, n = 15 (mean ± S.E). Data were compared with Mann-Whitney Rank Sum test. No significant differences were detected).

To quantify the extent of GIRK inhibition by G_qPCR agonists, we measured GIRK current amplitudes immediately before and at the end of the agonist application. This current difference is indicated in Fig. 4C and D (upper traces) by the dotted lines and the red arrows referring to I_{inhib}. The fraction of agonist-inhibited GIRK current (I_{inhib}) was related to the amplitude of the GTPγ-S-induced GIRK current before application of agonists (termed I_0 and indicated by the black arrows in Fig. 4C,D). The extent of G_qPCR-induced PIP_2-depletion was analyzed by relating the agonist-induced change in FRET ratio at the end of agonist application (dotted lines and red arrows in Fig. 4C,D, lower traces) to the maximal Ci-VSP-induced PIP_2-depletion (black arrows). Data summarizing the extent of G_qPCR-induced GIRK current inhibition and PIP_2-depletion are shown in Fig. 4E. These data indicate that endogenous atrial α_1-AR and endothelin receptors have similar efficiencies of inducing PIP_2-depletion. Obviously, receptor-specific differences in α_{1B}-AR- or ET-receptor induced GIRK inhibition in rat atrial myocytes (see Fig. 1) are not attributable to receptor species-dependent modulation of membrane PIP_2. Since stimulation of G_qPCRs activates both branches of downstream G_q signalling pathways, the question arises if receptors-specific activation of PKC determines the receptor-dependent extent of GIRK inhibition.

3.3. G_qPCR-independent GIRK inhibition by PKC activation

To address the contribution of PKC activation to GIRK inhibition, we analyzed the modulation of GTPγ-S-induced GIRK currents by the PKC activator Phorbol 12-myristate 13-acetate (PMA) and simultaneously monitored membrane PIP_2 in Ad-PIP_2-tool infected myocytes. Concomitantly, we monitored signalling-independent changes in membrane PIP_2 during activation of Ci-VSP. Exposure to PMA (200 nmol/L) resulted in a gradual decline of the GTPγ-S-activated current to a steady-state level (Fig. 5A, upper trace) which was not accompanied by a simultaneous change in membrane PIP_2. Voltage activation of Ci-VSP in the presence of PMA caused additional inhibition of current, paralleled by a change in the FRET trace, ruling out that a reduction in sensitivity of the biosensor accounts for the loss in correlation between membrane PIP_2 and current inhibition during PMA application (Fig. 5A, lower trace and summarized data in Fig. 5C). This clearly suggests that a sizable fraction of GIRK current inhibition by activation of the G_q/PLC pathway does not directly reflect depletion of PIP_2, but depends on PKC activation.

Consistent with these results, pharmacological block of PKC by the nonspecific PKC inhibitor chelerythrine (0.5 μmol/L, incubation for 1 h) almost completely abolished PMA-induced GIRK inhibition (Fig. 5B). As shown in the representative current trace in Fig. 5B and in the summarized data in Fig. 5C, chelerythrine in the absence of PMA had no effect on GTPγ-S-activated GIRK currents, thus excluding a putative nonspecific interference with GIRK channels. However, in the continuous presence of chelerythrine, GIRK inhibition by PMA was markedly diminished (Fig. 5B and C). The quantitatively minor effects of direct PKC activation on GIRK activity (about 30% inhibition, Fig. 5C) as compared to the pronounced inhibitory effects of G_qPCR agonists (about 50% inhibition, Fig. 4E) might be expected if only one branch of downstream G_q signalling pathways (here PKC) is activated. Accordingly, neither treatment with PMA nor chelethyrine induced a detectable depletion of membrane PIP_2. Importantly, the presence of both substances did not affect the dynamics of the PIP_2 pool, as activation of Ci-VSP caused robust PIP_2-depletion and subsequent changes in the FRET response of the PIP_2 biosensor.

3.4. Contribution of PKC isoforms to α_{1B}-AR- and ET-R-induced GIRK inhibition

Both *conventional* PKC isoforms (cPKCs, Ca^{2+}- and DAG-dependent) and *novel* PKC isoforms (nPKCs, DAG-dependent, but Ca^{2+}-independent) are downstream effectors of G_q-coupled receptor signalling pathways, but their contribution to GIRK channel modulation is still controversial [19,20,37]. We focused our interest on a possible contribution of cPKCs to GIRK channel modulation since a recent study described the inhibitory effect of PKCα, PKCβ1 and PKCβ2 on $IK_{(ACh)}$ in inside-out cell free patches [37]. Since GIRK channels are vulnerable to signal-independent, direct inhibition by a wide range of substances, e.g.

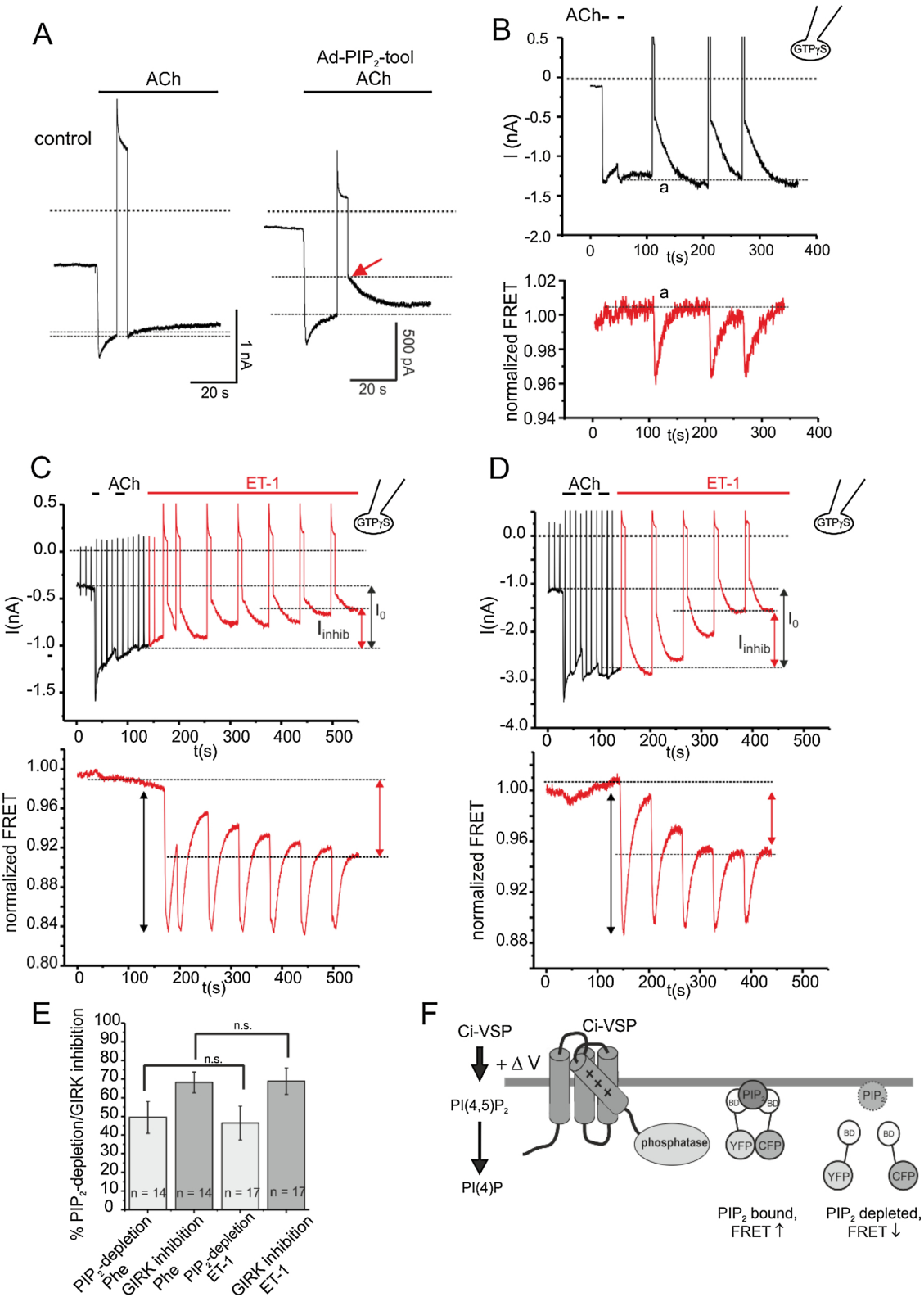

(caption on next page)

Fig. 4. Reducing membrane PIP_2 by voltage-dependent activation of Ci-VSP or by G_qPCR stimulation inhibits atrial GIRK channels.
A. Representative current recordings of ACh-activated (10 μmol/L) GIRK currents in native (left trace, n = 5) or Ad-PIP_2-tool-infected atrial myocytes (right trace, n = 7). Note that activation of Ci-VSP (by a test pulse from −90 mV to +60 mV for 4 s) instantaneously inhibited $IK_{(ACh)}$ (indicated by the arrow). B. Simultaneous patch-clamp and FRET recordings of GTPγ-S-activated GIRK currents during activation of Ci-VSP. Note that the PIP_2 depletion/resynthesis and GIRK current inhibition/recovery had the same time course (indicated by lower case "a").
Representative patch-clamp and FRET recordings of GTPγ-S-activated GIRK currents in Ad-PIP_2-tool-transfected atrial cells during application of Phe (C, 100 μmol/L) or ET-1 (D, 10 nmol/L). Dotted lines and red arrows indicate the level of Phe/ET-1-induced reduction in GIRK amplitude (upper traces) or reduction in membrane PIP_2 (lower traces) at the end of agonist application as compared to the GIRK current in the absence of GqPCR agonists or to the maximal Ci-VSP-induced PIP_2-depletion (−90 mV to +60 mV for 8 s) (black arrows). Membrane currents in response to depolarizing voltage ramps are shown as upward deflections.
E. Summarized data of G_qPCR-induced GIRK inhibition and PIP_2-reduction. Agonist-induced current inhibition was determined by evaluating GIRK amplitudes before (I_0) and at the end of agonist application (I_{inhib}). PIP_2-reduction was evaluated by relating the agonist-induced decrease of the FRET ratio (indicated by red arrows in the lower traces of C and D) to the maximal Ci-VSP-induced decrease of the FRET ratio (black arrows, lower traces in C and D). Significance was tested by Student's t-Test. n.s. not significant.
F. Scheme of the Ad-PIP_2-tool monitoring PIP_2-depletion during activation of Ci-VSP. The phosphatase activity of Ci-VSP is activated upon depolarization (indicated by +ΔV) and depletes membrane PIP_2 without activating PLC-mediated downstream signalling pathways.

[38–40], we tested all pharmacological PKC inhibitors in terms of their ability to induce nonspecific effects on GIRK activity. As a rule, GTPγ-S-activated currents were monitored during long-lasting application of ACh (10 μmol/L) in the presence and absence of different PKC inhibitors. As indicated by the summarized data in Fig. 6C,F and I , all PKC inhibitors used in the present study are devoid of nonspecific inhibitory effects. In general, atrial myocytes were incubated for 2 h with the respective PKC inhibitors which were also present in the recording solutions throughout the experiments.

In a first series of experiments, we incubated atrial myocytes with the PKC inhibitor Gö6976, which inhibits the cPKC isoforms PKCα and PKCβI with an IC_{50} of 2.3 nmol/L and 6.2 nmol/L without affecting the activity of PKCδ even at high concentrations in the micromolar range [41]. Thus, this inhibitor provides a reliable pharmacological tool to disrupt the activity of cPKCs and to dissect the contribution of cPKC isoforms to GIRK modulation.

Analogous to the experiments shown in Fig. 2C, coapplication of Phe (100 μmol/L) and ACh (10 μmol/L) resulted in pronounced inhibition of GTPγ-S activated GIRK currents (Fig. 6A), which was significantly reduced in the presence of 10 nmol/L Gö6976 (Fig. 6B and summarized data in Fig. 6C). Since Gö6976 in a concentration of 10 nmol/L may partially inhibit PKCβ1 and PKCβ2, we investigated Phe-induced GIRK modulation in the presence of the PKC inhibitor Ro32–0432, that preferentially inhibits PKCα (IC_{50} = 9 nmol/L) over PKCβ (IC_{50} = 28 nmol/L [42]). In the continuous presence of Ro32-0432 (15 nmol/L), GIRK inhibition during stimulation of α-adrenergic receptors was further impeded (Fig. 6E,F). To evaluate the contribution of the Ca^{2+}-dependent PKC isoforms PKCβ1 and PKCβ2 to GIRK inhibition, we decided to use the PKC blocker Enzastaurine that selectively inhibits PKCβ with an IC_{50} of 6 nmol/L as compared to 39 nmol/L for inhibition of PKCα [43]. Interestingly, inhibition of PKCβ by 10 nmol/L Enzastaurine did not affect the α-adrenergic-induced inhibition of GTPγ-S-activated GIRK currents (Fig. 6G-I), supporting the notion that $α_1$-receptor-specific activation of PKCα, but not of PKCβ, contributes to GIRK modulation.

Analogous experiments were performed during coapplication of ET-1 (10 nmol/L) and ACh (10 μmol/L) in the presence and absence of PKCα and PKCβ inhibitors (Fig. 7). The representative current recordings in Fig. 7B and E indicate that pharmacological block of PKCα did not impede ET-1-induced GIRK inhibition (see also summarized data in Fig. 7C and F), but that selective inhibition of PKCβ almost abolished ET-1-induced GIRK current decay (Fig. 7H and summarized data in Fig. 7I).

The data presented so far strongly support the notion that α-adrenergic and ET-receptors modulate atrial GIRK channels by receptor-specific activation of different Ca^{2+}-dependent PKC isoforms rather than by receptor-dependent differences in membrane PIP_2 depletion.

3.5. PKC inhibition reduces the decline of DAG formation in HEK cells expressing $α_{1B}$- or ET_B-receptors

The question arises if receptor-specific recruitment of different PKC isoforms during G_qPCR stimulation might also modify the kinetics of signalling molecule formation downstream of G_q, e.g. by exerting a feedback regulation of receptor function.

To address this, we analyzed the $α_{1B}$-AR function by monitoring DAG formation with the DAGR-FRET biosensor in the presence and absence of different PKC inhibitors (Fig. 8). In these set of experiments, the duration of agonist application was prolonged to 180 s analogous to the experiments shown in Figs. 6 and 7. We determined the $α_{1B}$-AR-induced DAG signal as the ratio $FRET_{60s\ after\ peak}/FRET_{peak}$ and observed a decline in the presence of Phe (10 μmol/L) by about 37% (see Fig. 8A and summarized data in Fig. 8G,H). Specific inhibition of PKCα with Gö6976 (10 nmol/L) reduced the decay of DAG formation (to 12%) and significantly prolonged the DAG signal during stimulation of $α_{1B}$-receptors, indicating a reduction of homologous $α_{1B}$-AR-densensitization in the continuous presence of phenylephrine (Fig. 8C,H). Activation of $α_{1B}$-receptors in the presence of the PKCβ inhibitor Enzastaurin (10 nmol/L) resulted in DAG formation that rapidly declined to a similar rate as compared to control conditions (compare Fig. 8A and E, see also summarized data in Fig. 8H), suggesting that activation of PKCβ has a minor feedback effect on receptor activity.

As described above (see Fig. 3J), the decline of the DAG signal (determined as the ratio $FRET_{30s\ after\ peak}/FRET_{peak}$) during stimulation of ET_B-receptors was slower as compared to the rate of DAG decline during $α_{1B}$-AR-activation, thus reflecting receptor-dependent differences in acute receptor desensitization. Similar results were observed for the decline of $α_{1B}$-AR- and ET-1-induced DAG signals during long-lasting agonist exposure (> 120 s), indicating different ratios of $FRET_{60s\ after\ peak}/FRET_{peak}$ (see Fig. 8G and H).

During pharmacological inhibition of PKCβ by Enzastaurin, the decay of the DAG signal during ET_B-receptor stimulation was significantly prolonged and the ratio $FRET_{60s\ after\ peak}/FRET_{peak}$ decreased from 22% to 9% (compare Fig. 8B and F), suggesting relevant contribution of PKCβ activation to the time course of ET_B-receptor-induced signalling. In contrast, pharmacological disruption of PKCα activity by Gö6976 did not prolong the decline of the ET-1-induced DAG signal, but instead, increased the DAG decay (Fig. 8D and I). The data presented so far suggest, that receptor-specific activation of different PKC isoforms has a dual role in either modulating activity of GIRK channels and in regulating receptor activity as monitored by the time course of G_qPCR-induced signalling pathways.

3.6. Chelation of intracellular calcium by BAPTA prolongs DAG signals and enhances G_qPCR-induced GIRK inhibition

Since an increase in $[Ca^{2+}]_i$ is a prerequisite for the activation of Ca^{2+}-dependent PKC isoforms, receptor-dependent differences in the

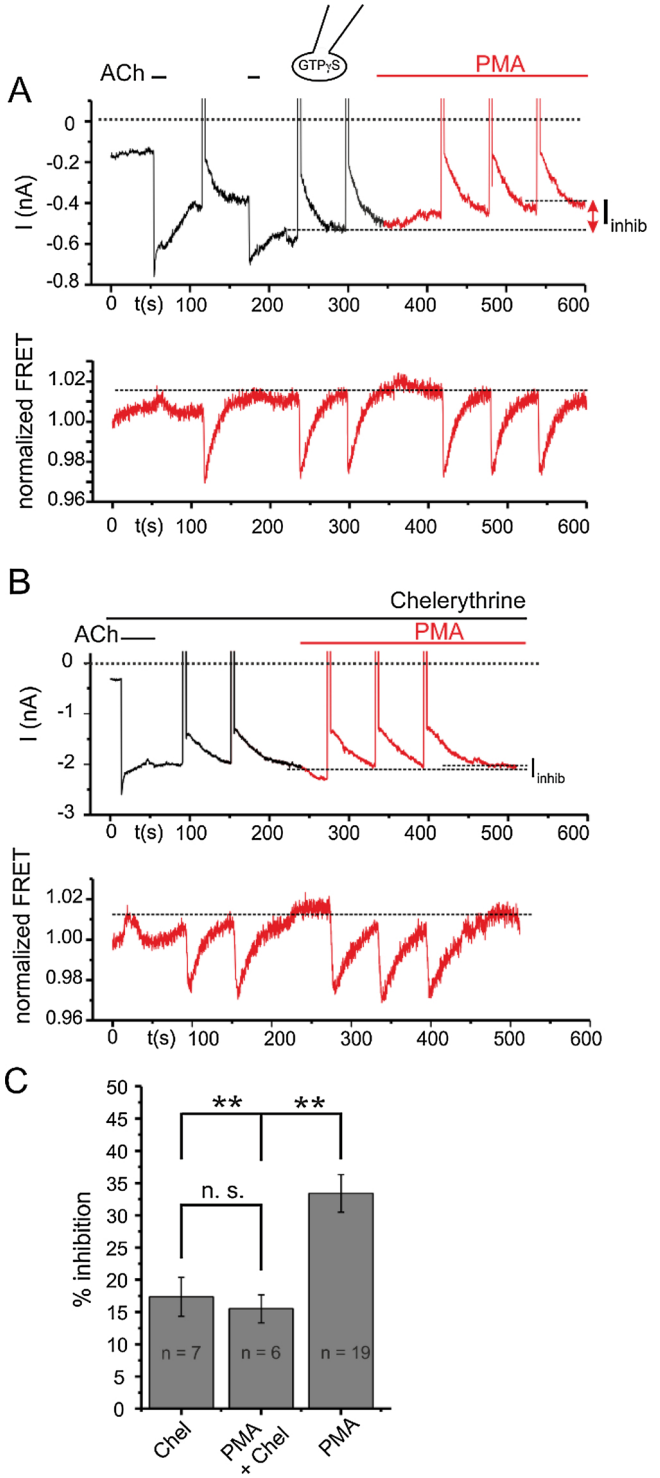

Fig. 5. PIP_2-independent GIRK inhibition is induced by PKC activation.
A/B. Representative patch-clamp and FRET recordings of GIRK currents and membrane PIP_2 in Ad-PIP_2-tool-infected atrial cells. A. Application of the direct PKC activator PMA (200 nmol/L) inhibited GIRK channel activity but failed to induce PIP_2-depletion. B. GIRK inhibition was reduced in the presence of the nonspecific PKC inhibitor chelerythrine (0.5 μmol/L, incubation for 1 h). C. Summarized data of GIRK inhibition in the presence of chelerythrine or PMA and during coapplication of chelerythrine and PMA. Significance ($p < 0.01$) between multiple groups was tested by One-way ANOVA and Holm-Sidak post-hoc test and marked by asterisks.n.s. not significant. Number (n) of experiments as indicated.

time course or amplitude of G_qPCR-induced $[Ca^{2+}]_i$ transients might induce recruitment of different cPKC isoforms during stimulation of α_{1B}-AR or ET-receptors. In a first series of experiments, we monitored the G_qPCR-induced increase in $[Ca^{2+}]_i$ in HEK 293 cells coexpressing either α_{1B}-AR or ET_B-R and the FRET biosensor Twitch-2B. The Twitch-2B biosensor has a minimal calcium binding motif based on the C-terminal domain of *Opsanus tau* Troponin C which is framed by a donor and an acceptor fluorescent protein and responds to Ca^{2+}-binding with an increase of the FRET ratio [30].

As depicted in the summarized FRET recordings in Fig. 9A and B , activation of α_{1B}-AR- or ET_B-R-induced a rapid increase of the FRET signal (reflecting the rise in $[Ca^{2+}]_i$) that rapidly declined in the presence of agonists. The decline of $[Ca^{2+}]_i$-transients during stimulation of α_{1B}-AR and ET_B-R had almost identical time courses as quantified by the ratio $FRET_{30s\ after\ peak}/FRET_{peak}$ (see Fig. 9Ca), indicating similar time courses of Ca^{2+} extrusion and sarcolemmal Ca^{2+} removal. However, we observed receptor-species dependent differences in the time course to reach peak $[Ca^{2+}]_i$ as indicated by the half time $t½ = 12.4 \pm 2.8$ s during α_{1B}-AR activation and $t½ = 6.5 \pm 0.7$ s, mean ± S.E.) during ET_B-R stimulation (Fig. 9Cb). Furthermore, the amplitude of the ET-1-induced FRET signal was significantly larger than the Phe-induced signal (Fig. 9A and B, indicated by asterisks in 9B). Given the large dynamic range of Twitch-2B and its linear response properties [30], these differences in the amplitude of the FRET signal might reflect receptor-specific efficiencies for raising $[Ca^{2+}]_i$.

The effect of receptor-species dependent recruitment of cPKCs on both GIRK activity and homologous receptor desensitization should be impeded by preventing the G_qPCR-induced rise in $[Ca^{2+}]_i$. To evaluate G_qPCR-induced GIRK inhibition under conditions that bypass the activation of cPKCs, we supplemented the pipette solution with the Ca^{2+}-chelator BAPTA (5 mmol/L) and measured the amplitude of ACh-activated GIRK currents in the presence of Phe or ET-1. As compared to the experiments recorded under control conditions (with GTP in the pipette solution, see Fig. 9D and G), GIRK inhibition during application of Phe or ET-1 was significantly increased in cells loaded with BAPTA (Fig. 9E and H). From the summarized data in Fig. 9F and I that show G_qPCR-induced GIRK inhibition under different recording conditions it is evident that both GTPγ-S and BAPTA augment the inhibitory effect during α_{1B}-AR- or ET-R activation.

At first sight, the pronounced GIRK current inhibition in the presence of BAPTA seems to be in conflict with the idea that activation of Ca^{2+}-dependent PKC isoforms significantly contribute to GIRK inhibition. Chelation of intracellular calcium should prevent the activation of cPKCs and reduce the extent of GIRK inhibition. On the other hand, the absence of cPKC activation might attenuate homologous receptor desensitization, thus resulting in prolonged receptor activity with pronounced PIP_2-depletion.

To monitor homologous desensitization of α_{1B}-AR activity in the presence of different pipette solutions, we transfected HEK 293 cells with α_{1B}-AR and DAGR and subsequently monitored the time course of DA G formation and DAG decay. We dialyzed α_{1B}-AR/DAGR-co-transfected HEK cells with a GTP (25 μmol/L)-containing pipette solution or with GTPγ-S (0.5 mmol/L) or with the Ca^{2+} chelator BAPTA (5 mmol/L) via the patch pipette and measured the time course of DAG decay in the presence of 10 μmol/L Phe. The traces in Fig. 9J represent the summarized and normalized FRET signals obtained under different recording conditions. As depicted in Fig. 9J, loading the cell with GTPγ-S or buffering the increase in $[Ca^{2+}]_i$ with BAPTA abolished the acute phase of DAG decline and prolonged Phe-induced DAG formation.

Prolonged DAG signals in the presence of GTPγ-S should be attributed to persistent activation of G proteins and signalling pathways downstream of G_q, notably PLC activation. As a consequence, the sustained DAG formation in the presence of GTPγ-S impedes the typically rapid decay of DAG production that is attributed to the rapidly desensitizing activity of α_{1B}-ARs.

In the presence of BAPTA in the pipette solution, Phe-induced DAG

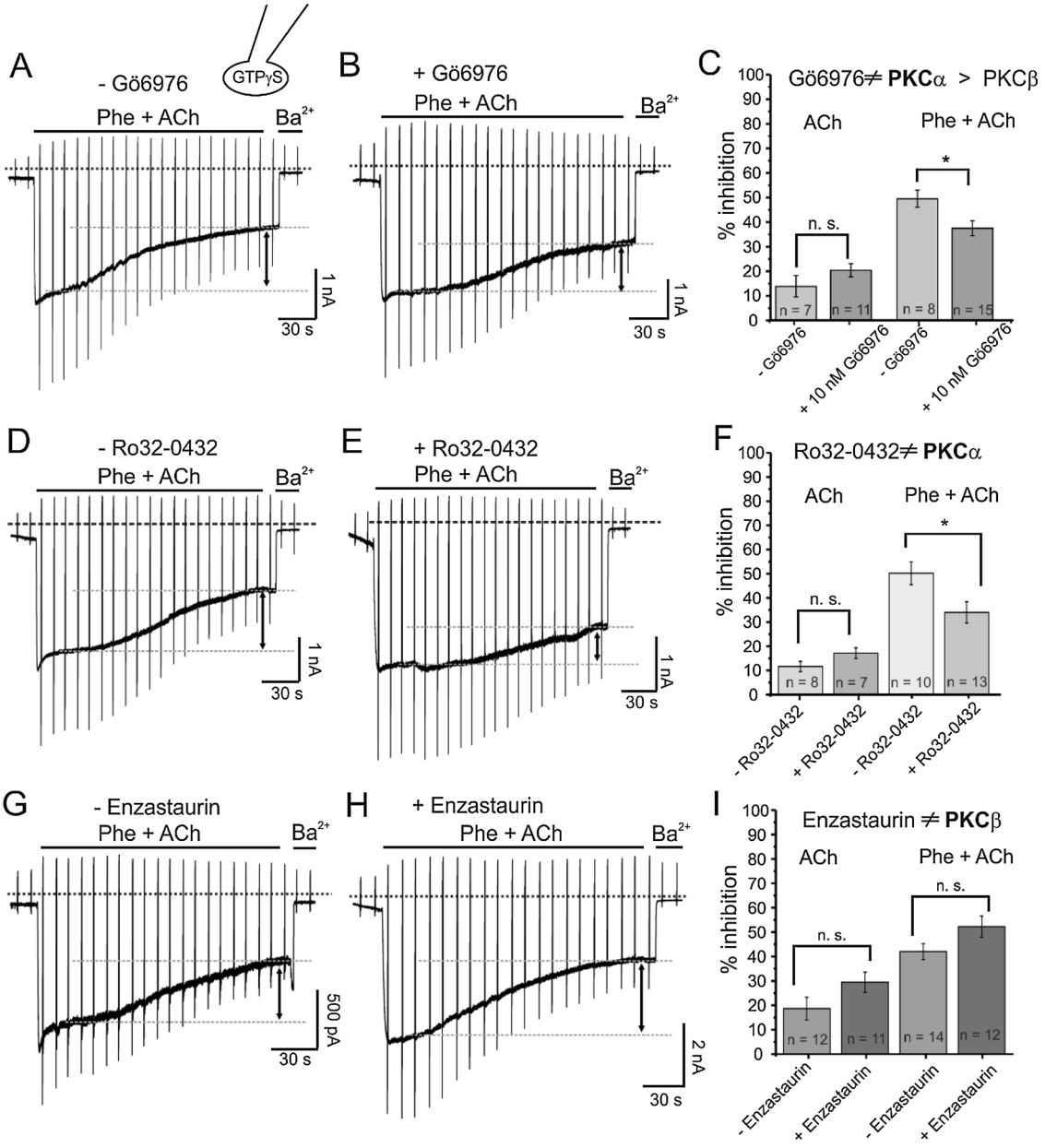

Fig. 6. Selective block of PKCα reduces Phe-induced GIRK inhibition.

A/B. Membrane recordings of GTPγ-S-activated GIRK currents during coapplication of Phe (100 μmol/L) and ACh (10 μmol/L) in the presence (B) and absence (A) of Gö6976 (10 nmol/L, 2 h incubation time). Gö6976 was present throughout the experiment. As a rule, atrial myocytes were incubated for 2 h and PKC inhibitors were present in the recording solution.

C. Summarized data of GIRK inhibition during application of ACh (10 μmol/L) alone or during coapplication of Phe and ACh in the presence and absence of Gö6976. Statistical significance was tested with the Mann-Whitney test (ACh +/− Gö) or Student's t-Test (Phe + ACh in the presence and absence of Gö). Significance of $p < 0.05$ is marked by an asterisk. n.s. not significant.

D/E. Recordings of GTPγ-S-activated GIRK currents during coapplication of Phe (100 μmol/L) and ACh (10 μmol/L) in the presence (E) and absence (D) of the specific PKCα inhibitor Ro32–0432 (15 nmol/L). F. Summarized data of GIRK inhibition in the presence and absence of Ro32–0432. Statistical significance was tested with Student's t-Test. Significance of $p < 0.05$ is marked by an asterisk. n.s. not significant. G/H. Recordings of GTPγ-S-activated GIRK currents during coapplication of Phe (100 μmol/L) and ACh (10 μmol/L) in the presence (H) and absence (G) of the specific PKCβ inhibitor Enzastaurin (10 nmol/L). I. Summarized data of GIRK inhibition in the presence and absence of Enzastaurin. Statistical significance was tested with unpaired Student's t-Test. n.s. not significant. Number (n) of experiments is indicated throughout.

formation did not significantly decline in the presence of agonist, confirming our previous observation that inhibition of cPKCs eliminated acute desensitization of α_{1B}-ARs (see Fig. 8). Sustained α_{1B}-AR activity in the presence of BAPTA prolongs PLC activation and augments membrane PIP_2-depletion, thus resulting in pronounced GIRK inhibition despite disruption of cPKC activation.

However, the activity of diacylglycerol kinases (DGK) that degrade DAG to phosphatidic acid (PA) in a reaction that terminates DAG-based signals, is also regulated by intracellular calcium (for review see [44]). Therefore, it is conceivable that intracellular Ca^{2+} chelation by BAPTA impedes DGK activity. As a consequence, reduced DAG degradation should result in prolongation of the DAG FRET signals.

In agreement with the data shown in Fig. 8, we attribute the prolonged DAG signal in the presence of BAPTA to the absence of cPKC activation rather than to impaired DAG degradation. These data demonstrated prolongation of DAG signals by pharmacological inhibition

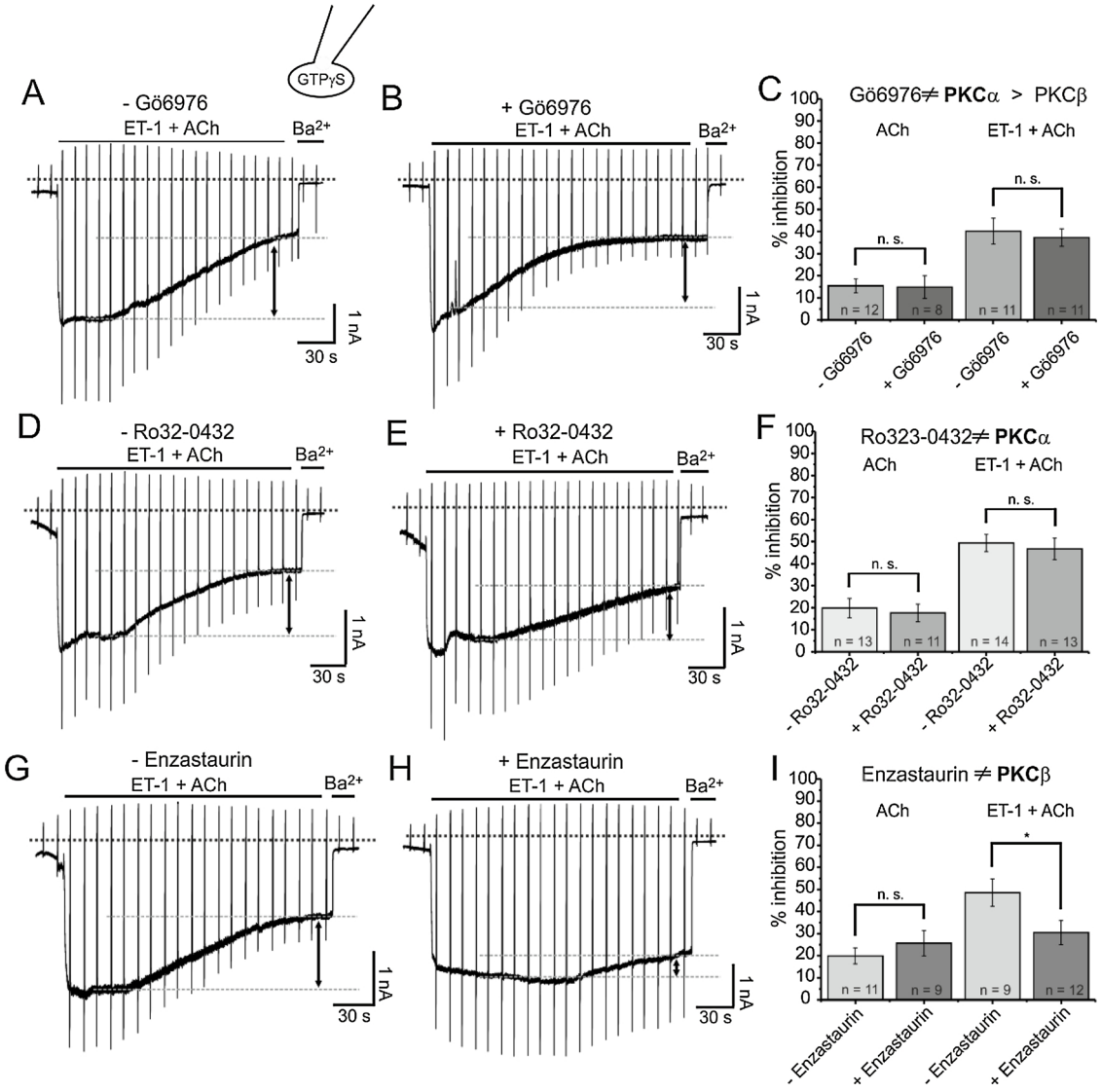

Fig. 7. Inhibition of PKCβ impedes ET-1-induced GIRK inhibition.
A/B. Whole cell patch-clamp recordings of GTPγ-S-activated GIRK currents during coapplication of ET-1 (10 nmol/L) and ACh (10 μmol/L) in the presence (B) and absence (A) of Gö6976 (50 nmol/L). C. Summarized data of GIRK inhibition in the presence and absence of Gö6976. Statistical significance between the means of two groups was evaluated with Student's t-Test (C,I and F(ACh ± Ro32–0432) and Mann-Whitney test (F, ET-1 + ACh ± Ro32–0432)). Significance of $p < 0.05$ is marked by an asterisk. Number (n) of experiments as indicated. n.s. not significant. D/E. Recordings of GTPγ-S-activated GIRK currents during coapplication of ET-1 and ACh in the presence (E) and absence (D) of Ro32–0432 (15 nmol/L) and summarized data of GIRK inhibition in the presence and absence of Ro32–0432 (F). G/H. Recordings of GTPγ-S-activated GIRK currents during coapplication of ET-1 (10 nM) and ACh (10 μM) in the presence (H) and absence (G) of the specific PKCβ inhibitor Enzastaurin (10 nmol/L) and summarized data of GIRK inhibition in the presence and absence of Enzastaurin (I).

of specific cPKC isoforms (Fig. 8C and F), indicating a significant contribution of Ca^{2+}-dependent PKCs to homologous receptor desensitization.

Assuming that the absence of cPKC activation eliminates homologous desensitization of G_qPCRs, it is tempting to speculate that overexpression of specific cPKC isoforms augments receptor-specific desensitization. To corroborate the important contribution of cPKCs to receptor desensitization, we probed α_{1B}-R and ET_B-receptor activity in the presence and absence of heterologously expressed PKC isoforms.

3.7. Expression of Ca^{2+}-dependent PKC isoforms augments receptor-specific desensitization in HEK293 cells

As shown in Figs. 6 and 7 of the present study, we dissected α_{1B}-AR- and ET-R-specific activation of different cPKC isoforms by using pharmacological inhibitors specific for PKCα or PKCβ that selectively impeded GIRK inhibition.

To address the contribution of these specific PKC isoforms to receptor activity and homologous desensitization, we aimed to monitor G_qPCR activity by means of a genetically encoded FRET-based biosensor that directly reports PKC activity (CKAR) [26,28]. The time course of the CKAR FRET signal is determined by phosphorylation of the CKAR substrate sequence and subsequently by phosphatase-dependent dephosphorylation of the substrate sequence [28]. Since PKC activity has been shown to critically depend on the G_qPCR-induced increase in $[Ca^{2+}]_i$ and DAG formation [26], receptor-dependent differences in the activation of signalling pathways downstream of G_q should result in distinct receptor-specific time courses of the CKAR signal.

We analyzed PKC activity in HEK293 cells coexpressing α_{1B}-AR or ET_B-R and CKAR to monitor receptor-specific differences during G_qPCR activation. Fig. 10A and B illustrate the summarized FRET recordings of PKC activity during receptor stimulation with Phe and ET-1. The CKAR FRET signal is displayed as the ratio F_{YFP}/F_{CFP}, thus a decrease of the

FRET signal corresponds to phosphorylation of the biosensor. The corresponding CKAR dynamics in α_{1B}-AR-expressing cells and ET_B-R transfected HEK cells display similar onset kinetics as quantified by the half times of FRET decrease during receptor stimulation ($t½ = 36.8 \pm 1.9$ s during activation of α_{1B}-receptors and $t½ = 31.6 \pm 2.02$ s during ET_B-R-stimulation, Fig. 10G and H, left-most bars). In the continuous presence of agonists, the CKAR signal decreased to a peak amplitude that was stable for at least 15 s

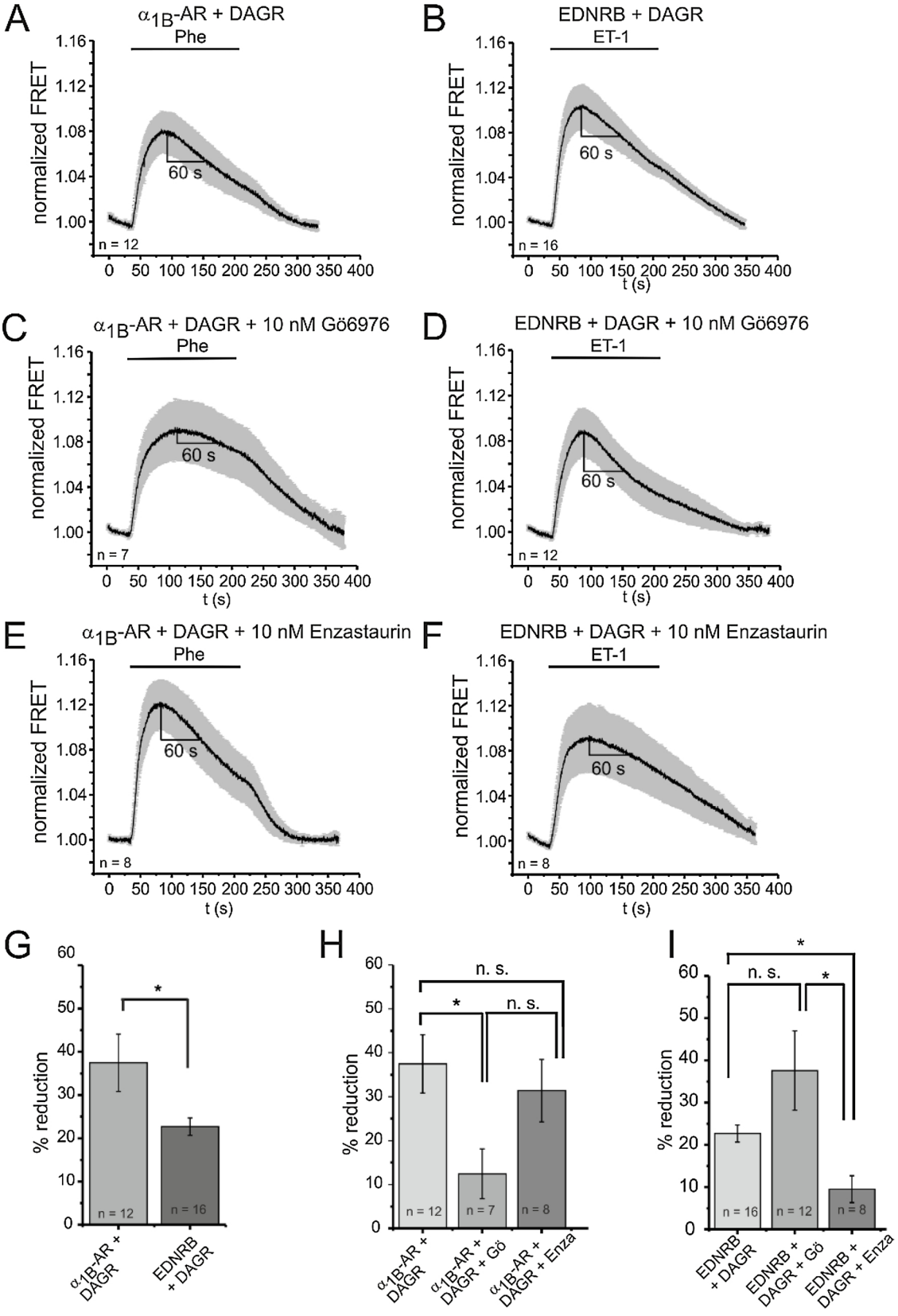

(caption on next page)

Fig. 8. Inhibition of Ca^{2+}-dependent PKC isoforms prolongs receptor-induced DAG signals in HEK293 cells.
A.C. Summarized FRET-recordings from α_{1B}-AR-expressing HEK 293 cells cotransfected with DAGR in the presence or absence (A) of Gö6976 (C) or Enzastaurin (E) (each 10 nmol/L, incubation time 2 h, inhibitors were present used throughout the experiment). Note that the decay of the DAG signal during stimulation of α_{1B}-AR (Phe 10 μmol/L, application time 180 s) was reduced by Gö6976, but not by Enzastaurin.
B,D,F. FRET-recordings from ETB-R-expressing HEK 293 cells cotransfected with DAGR in the presence (D,F) or absence (B) of Gö6976 or Enzastaurin (same concentrations and recording conditions as in C and E). G. Summarized data comparing DAG decline during Phe and ET-1 application defined as the ratio $FRET_{60s after peak}/FRET_{peak}$(corresponding leftmost bars in H and I). Significance was tested with Student's test. P-value less than < 0.05 was marked by an asterisk. H. Summarized data comparing DAG decline during Phe application defined as the ratio $FRET_{60s\ after\ peak}/FRET_{peak}$. Multiple group comparisons were assessed with One-way ANOVA and Holm-Sidak post hoc test. P-value less than < 0.05 was marked by an asterisk.
I. Summarized data comparing DAG decline defined as the ratio $FRET_{60s\ after\ peak}/FRET_{peak}$ during application of ET-1 (100 nmol/L). Multiple group comparisons were assessed with Kruskal-Wallis ANOVA and Dunn post hoc test. P-values < 0.05 were considered statistically significant and marked by asterisks. n.s. = not significant. Number (n) of experiments is indicated throughout.

(indicated by dotted lines in Fig. 10A and B) and then slowly declined to basal levels. To quantify the FRET decline, we evaluated the ratio $FRET_{30s\ after\ peak}/FRET_{peak}$ (see summarized data in Fig. 10I and J) and obtained similar values in α_{1B}-AR/CKAR- and ET_B-R/CKAR-expressing cells (about 20%, see leftmost bars in Fig. 10I and J).

Coexpression of PKCα or PKCβ1 in α_{1B}-AR/CKAR- or ET_B-R/CKAR-expressing HEK cells accelerated the initial decrease of the CKAR response during agonist application (Fig. 10C–F) maybe as a result of higher total PKC expression (see also summarized data in Fig. 10G and H).

However, the decline of the CKAR signal during sustained agonist application (> 100 s) was significantly accelerated upon coexpression of cPKCs, depending on the G_qPCR species and cPKC isoform (see summarized data in Fig. 10I and J). The decay of the Phe-induced CKAR signal was increased with coexpression of PKCα, but not with PKCβ1 (Fig. 10C,E) whereas the CKAR signal in ET_B-R/CKAR-expressing HEK cells rapidly declined upon coexpression of PKCβ1, but not of PKCα (Fig. 10D,F).

Since the time course of the CKAR signal is related to receptor-specific formation of signalling molecules downstream of G_q, differences in the onset and decay of the signal should be directly related to distinct receptor activity. The initial onset of the CKAR signal has been attributed to an increase in $[Ca^{2+}]_i$ whereas the late phase of the PKC response depends on sustained DAG production [26]. Since the duration of the CKAR signal is controlled by the DAG turnover, increased receptor desensitization that confines the formation of DAG should reduce the duration of the FRET signal.

Thus, the receptor-specific and cPKC isoform-dependent modulation of the CKAR FRET signal indicates the feedback modulation of receptor activity and homologous desensitization of G_qPCR receptors. From the experiments presented above, we can conclude that homologous desensitization of α_{1B}-AR is increased by PKCα whereas PKCβ1 augments desensitization of ET_B-R, suggesting a novel role of receptor-specific activation of different cPKC isoforms in regulating receptor activity.

4. Discussion

In the present study, we investigated receptor-specific signalling of α-adrenergic and endothelin ET-receptors as paradigmatic G_q-coupled receptors that have been shown to modulate cardiac function by strong inhibition of atrial GIRK currents [2,5]. By investigating the activity of atrial GIRK channels as effector proteins of $G_{i/o}$- and G_q-induced signalling pathways, we were able to elucidate receptor-specific coupling of endogenous α_1-AR and ET-receptors to specific cPKC isoforms and to evaluate the efficiency of G_qPCR agonists to inhibit GIRK currents. Furthermore, the data presented in this study suggest a novel role of receptor-specific activation of different cPKC isoforms in regulating both effector and receptor activity via a negative feedback mechanism that augments homologous receptor desensitization.

We focused our interest on the downstream G_q signalling of α-adrenergic and endothelin ET-receptors since these receptors exhibit some interesting intrinsic characteristics that might account for different receptor-specific spatiotemporal signalling. As confirmed in a recent study [24], rapid densitization of α_{1B}-adrenergic receptors (α_{1B}-AR) modulates effector activity (therein I_{Ks}) by restricting the spatiotemporal activation of downstream G_q signalling components, more precisely, by controlling PIP_2-reduction and recruitment of different PKC isoforms, thus resulting in different modes of fine-tuning of I_{Ks} activity. Furthermore, this study provided evidence that Ca^{2+}-dependent PKCs contribute to homologous α_{1B}-AR-desensitization since inhibition of cPKCs abolished α_{1B}-AR-desensitization.

An intrinsic feature of endothelin receptors is the stimulation-induced receptor recruitment to caveolae and the formation of ET-receptors /GIRK channel signalling complexes in these microdomains [9]. ET-receptor specific effects on GIRK activity critically depend on the restricted diffusion of PIP_2 and on the confined PIP_2-depletion in close proximity to the colocalized ET-receptor/GIRK channels. It is conceivable that the final spatial control of PIP_2-signalling during activation of ET-receptors might account for the marked GIRK inhibition in the present study as compared to α_{1B}-induced GIRK inhibition (see Fig. 1). However, several lines of evidence support our idea that α_{1B}- and ET-receptor-specific differences in GIRK inhibition are based primarily on specific recruitment of cPKC isoforms rather than on receptor-specific control of PIP_2-depletion.

First, as indicated by the data in Fig. 4, endogenous atrial α_1-AR and endothelin receptors have similar efficiencies of inducing membrane PIP_2-depletion. Second, we observed significant receptor-specific reduction of G_qPCR-induced GIRK inhibition by using selective pharmacological blockers of different cPKC-isoforms demonstrating activation of PKCα during stimulation of α_1-AR (Fig. 6) and activation of PKCβ isoforms during ET-receptor-stimulation (Fig. 7).

Inhibition of one branch of the signalling pathway downstream of G_q by pharmacological disruption of PKC activity should unmask the contribution of PLC activation and PIP_2-depletion to GIRK inhibition. However, we did not observe any receptor-specific differences in the extent of GIRK inhibition in the presence of Ro32–0432 or Enzastaurin (compare Fig. 6F, Phe/ACh + Ro32–0432 and Fig. 7I, ET-1/ACh + Enzastaurin). These experiments exclude receptor-dependent differences in membrane PIP_2-depletion as the underlying mechanism of receptor-specific GIRK inhibition in rat atrial myocytes.

As described in the introduction, only few studies investigated receptor-specific PKC signalling and subsequent regulation of GIRK channel activity. In hippocampal CA1 neurons, receptor-specific inhibition of neuronal GIRK channels comprises muscarinic receptor-induced activation of the PLC/PKC signalling pathway but activation of the phospholipase A2/arachidonic acid pathway during stimulation of metabotropic glutamate receptors (mGluR [8]). This receptor-specific crosstalk between G_qPCRs and neuronal GIRK channels is not directly applicable with the idea of receptor-specific spatial organization of signalling components, since in this study inhibition of neuronal GIRK channels is attributed to the activation of different signalling pathways [8].

The contribution of different PKC isoforms to GIRK channel activity has been investigated in atrial myocytes derived from untreated and atrial tachypaced dogs [37]. This study demonstrated GIRK inhibition by conventional Ca^{2+}-dependent PKC isoforms (cPKCs) and GIRK

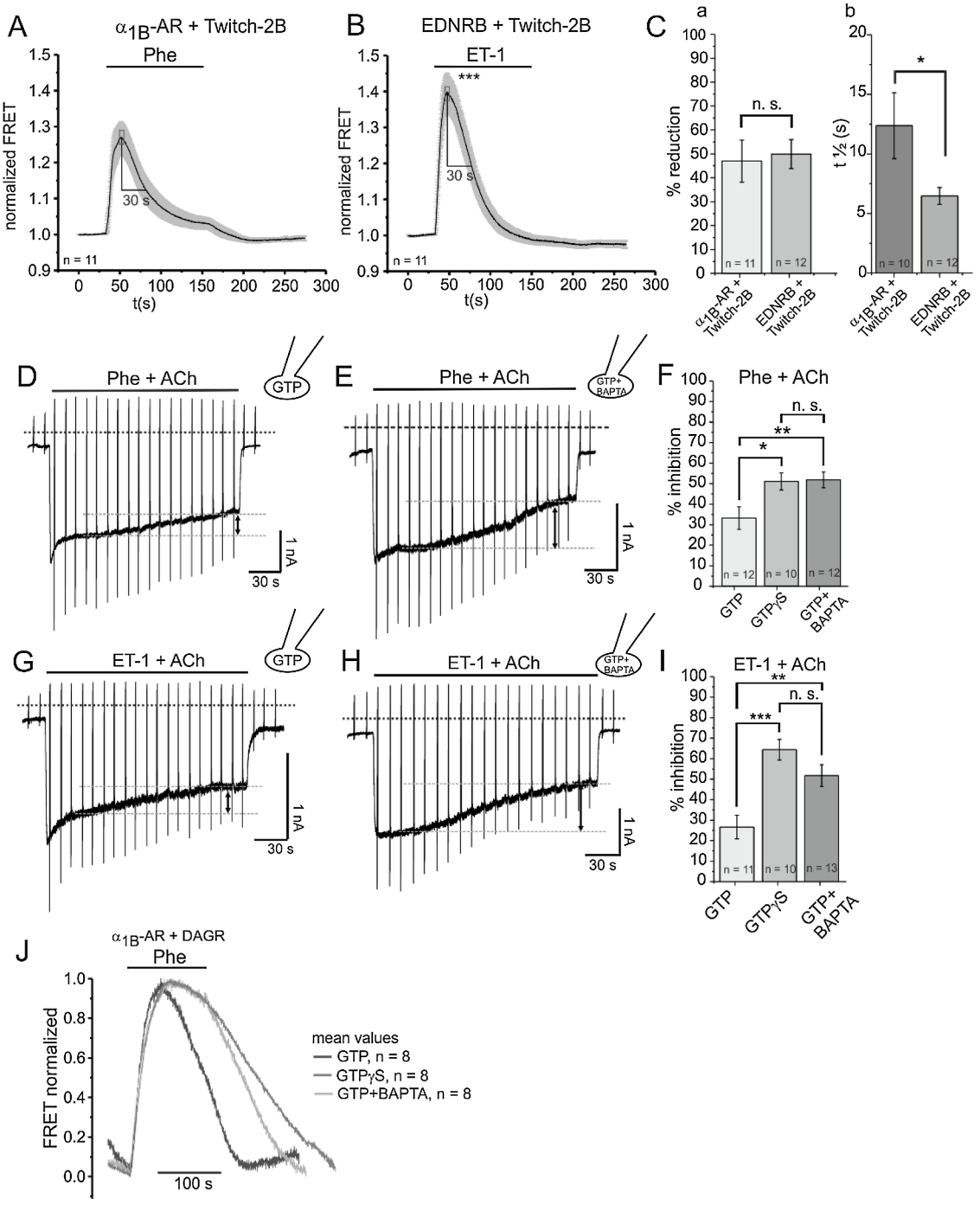

Fig. 9. Chelation of intracellular Ca^{2+} augments Phe- and ET-1-induced inhibition of GIRK currents.

A.B. Summarized FRET recordings monitoring the increase in $[Ca^{2+}]_i$in α_{1B}-AR or ET_B-R and Twitch-2B cotransfected HEK cells during agonist application (Phe 10 μmol/L, ET-1100 nmol/L). Mean peak data within a time frame of 5 s (corresponding 25 data points), indicated by grey boxes, were compared by Student's t-Test. $P < 0.001$ was marked by asterisks. C(a). Summarized data evaluating the decline of the FRET signal in the presence of G_qPCR agonists as indicated by the ratio $FRET_{30\ after\ peak}/FRET_{peak}$. Mann-Whitney test was used to evaluate significant differences between two groups. n.s. not significant. C(b). Summarized data evaluating the half time (t½) of the increase in FRET during application of Phe or ET-1. Significance was tested by the Mann-Whitney test and $p < 0.05$ is marked by an asterisk. D,G. Representative current recordings of ACh-activated (10 μmol/L) GIRK currents in the presence of phenylephrine (100 μmol/L, D) or ET-1 (10 nmol/L, G) recorded with the standard pipette solution ("GTP") E,H. Representative GIRK currents during coapplication of ACh and phenylephrine or endothelin (same concentrations as in D and G). Cells were dialyzed with a pipette solution containing 5 mmol/L BAPTA ("GTP + BAPTA").

F,I. Summarized data indicating GIRK inhibition by Phe or ET-1 under different recording conditions. Inhibition was quantified as indicated by the arrows in D-H. One-way ANOVA and Holm-Sidak test were used for multiple group comparisons. Significance of $p < 0.05$ is marked by an asterisk, $p < 0.01$ by two and $p < 0.01$ by three asterisks. J. Summarized FRET recordings (mean values) in HEK 293 cells cotransfected with α_{1B}-AR and DAGR to monitor DAG formation in the presence of 1 μmol/L Phe. Cells were dialyzed with different pipette solutions as indicated.

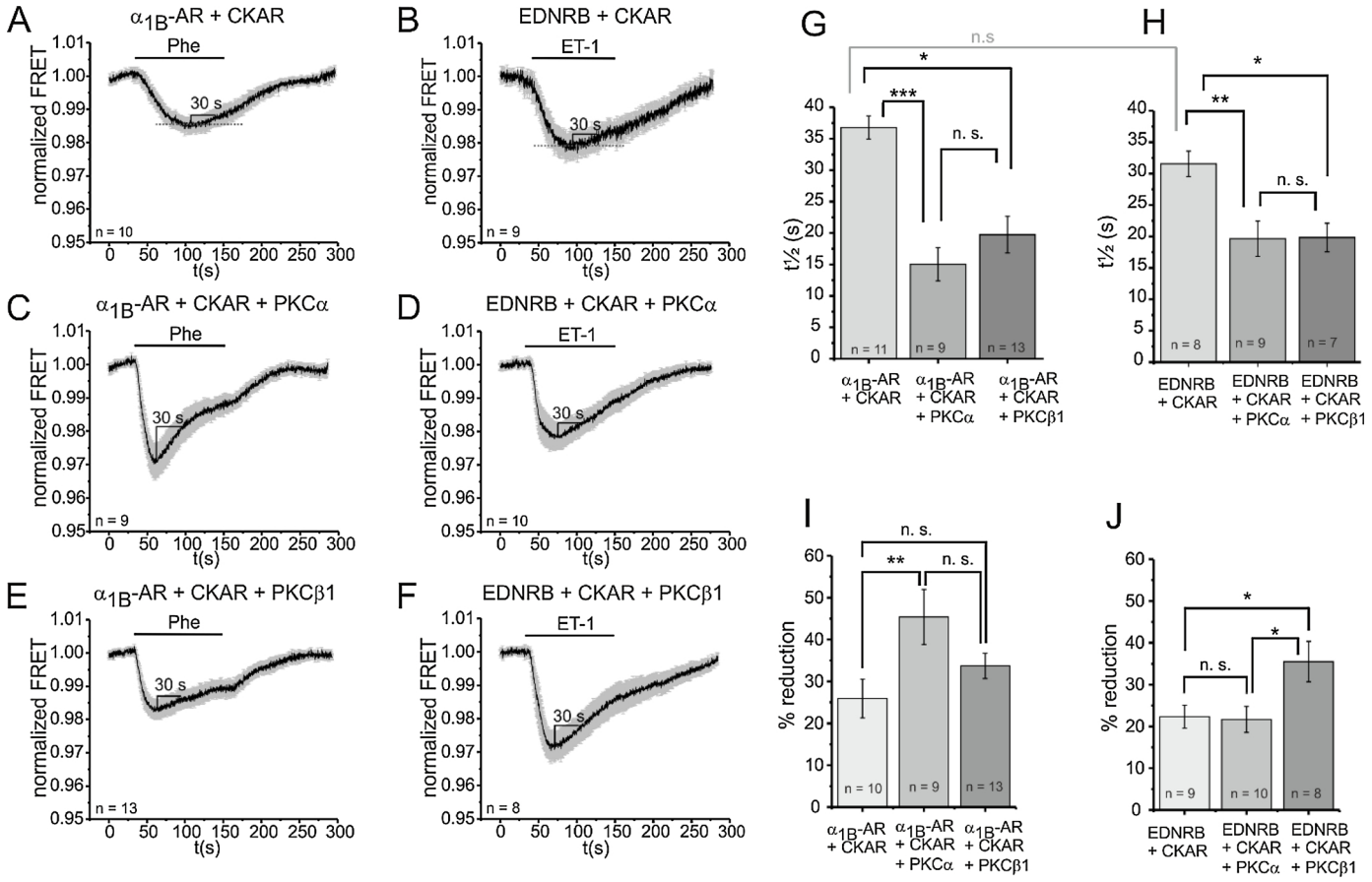

Fig. 10. Modulation of G_qPCR-induced CKAR signals in HEK293 cells by coexpression of specific cPKC isoforms.
A.B. FRET recordings from α_{1B}-AR/CKAR- (A) or ET_B-R/CKAR expressing HEK293 cells (B) during application of Phe (120 s, 10 μmol/L) or ET-1 (100 nmol/L). Recordings are illustrated as mean values ± S.E. Peak amplitudes of FRET signals are indicated by dotted lines. C.D. Summarized FRET recordings from $_{\alpha 1B}$-AR/CKAR- (C) or ET_B-R/CKAR expressing HEK293 cells (D) cotransfected with WT-PKCα in the presence of Phe and ET-1 (same concentrations as in A and B). E.F. Summarized FRET recordings from α_{1B}-AR/CKAR- (E) or ET_B-R/CKAR expressing HEK293 cells (F) cotransfected with WT-PKCβ1 in the presence of Phe and ET-1 (same concentrations as in A and B). G.H. Summarized data comparing the onset kinetics (half times, t½) of FRET signals in α_{1B}-AR/CKAR- and ET_B-R/CKAR-expressing cells (corresponding Fig. 10A–F). Kruskal-Wallis ANOVA and Dunn post-hoc test were applied for group comparisons. Student's t-Test was used for comparing t½ of α1B-AR and ETB-R-induced CKAR signals without coexpression of PKCs (see leftmost bars in G and H, indicated by the grey line). I.J. Summarized data comparing the decline of the CKAR signal during agonist application (determined by the ratio $FRET_{30s\ after\ peak}/FRET_{peak}$). One-way ANOVA and Holm-Sidak test were used for multiple group comparisons. P-values < 0.05 were considered significant and marked by one asterisk, $p < 0.01$ by two asterisks and $p < 0.001$ by three asteriks. n.s. not significant. Number (n) of experiments is indicated throughout.

activation by novel (Ca^{2+}-independent) PKC isoforms (nPKCs) in both control and in ATR (atrial tachycardia-induced remodeling) myocytes. By comparing the PKC isoform expression in control versus ATR cardiomyocytes, a significant reduction in the expression level of the cPKC isoform PKCα was found, whereas the expression of other PKC isoforms (PKCβ1,PKCδ,PKCε) in ATR cardiomyocytes was unchanged. However, immunoblot experiments on separated cytosolic and membrane fractions indicated that the relative expression of the nPKC isoform PKCε in the membrane fraction was significantly increased in ATR cells, pointing to translocation of PKCε from the cytosol to the cell membrane. The authors conclude that atrial tachycardia is associated with increased constitutive GIRK currents according to downregulation of cPKCs and increased membrane localization of nPKCs, thus shifting the balance of PKC effects towards enhanced GIRK activity [37].

By using specific pharmacological tools (Figs. 6 and 7), we were able to dissect the contribution of different PKC isoforms to α_{1B}-AR- and ET-R-induced effector modulation, supporting the notion that cPKCs rather than nPKCs contribute to inhibition of GIRK channel activity in native atrial myocytes.

It was beyond the scope of the present study to elucidate the molecular mechanism of cPKC-induced GIRK inhibition with regard to either PKC-induced reduction of GIRK affinity to PIP_2 [10,15,16] or to direct contribution of phosphorylated GIRK residues to channel gating as described recently for Kir.3.2 channels [14]. Furthermore since PKC activation is concomitant with PIP_2-hydrolysis, it is difficult to dissect PKC effects versus PIP_2-depletion and to determine a receptor-specific hierarchy of G_qPCR-induced channel regulation. The experiments shown in Fig. 5 suggest a quantitatively minor effect of direct PKC activation by PMA on GIRK activity (Fig. 5C) as compared to the pronounced inhibitory effects of G_qPCR agonists (Fig. 4E), suggesting that both branches of downstream G_q signalling pathways need to be activated to exert maximal channel inhibition.

However, we attribute the different efficiencies of α_1-AR and ET-R to induce GIRK inhibition (see Fig. 1) to receptor-specific differences in homologous desensitization that controls the duration and the specificity of PKC activation. As indicated by the FRET measurements with the biosensor DAGR (Fig. 3) which is a reliable tool to study the time course of G_qPCR desensitization by dynamic DAG formation [35], we were able to correlate the time courses of the α_{1B}-AR- and ET-R-induced DAG signals to different rates of receptor desensitization. Prolonged DAG formation and the significantly slower decay of the DAG signal during ET-R stimulation should result in sustained PKC activation whereas the corresponding DAG dynamics during α_{1B}-AR activation showed a more rapid decline during agonist application thus limiting downstream PKC

activation. Receptor-dependent differences in spatiotemporal activation of downstream G_q signalling components are also evident from the data shown in Fig. 10, reporting PKC activation with the FRET biosensor CKAR.

Although in a previous study the FRET-reporter system CKAR has been suspected to be saturated by small amounts of DAG thus impeding the investigation of receptor-specific efficiencies of PKC activation [45], we frequently observed receptor-species-dependent differences in the time course and amplitude of the CKAR signal (Fig. 10A and B). Since the late phase of the CKAR response depends on sustained DAG production [26], pronounced PKC activation during ET-receptor activation is compatible with prolonged DAG formation according to delayed ET receptor desensitization. However, since the CKAR sensor is phosphorylated by all conventional and novel protein kinase C isozymes tested [46], it is not applicable to report the activation of specific PKC isoforms during α_{1B}-AR and ET-R-induced signalling.

Several lines of evidence support the idea that receptor-specific activation of either PKCα and PKCβ modulates the duration of receptor activity and as a consequence the time course of the CKAR signal.

Receptor activity, as monitored by DAG formation, was significantly prolonged in the presence of the Ca^{2+}-chelator BAPTA (Fig. 9J), pointing out a contribution of Ca^{2+}-dependent effector proteins to homologous receptor desensitization. Considering the fact that chelation of intracellular Ca^{2+} with BAPTA inhibits a variety of Ca^{2+}-dependent signalling pathways and effector proteins, prolongation of DAG signals might also be induced by impaired activity of diacylglycerol kinases (DGKs). However, we attribute the prolonged DAG signal in the presence of BAPTA to the absence of cPKC activation rather than to impeded DAG degradation. This notion is supported by the experiments shown in Fig. 8, indicating that pharmacological inhibition of specific cPKC isoforms determines the time course of G_qPCR-induced DAG signals. More precisely, pharmacological inhibition of PKCα eliminated desensitization of α_{1B}-ARs and prolonged DAG formation (Fig. 8C) whereas inhibition of PKCβ significantly reduced homologous desensitization of ET_B-receptors (Fig. 8F).

In line with the modulation of homologous receptor activity by specific cPKCs, we observed that coexpression of PKCα abbreviated the CKAR signal resulting from confined formation of signalling molecules downstream of α_{1B}-AR activation. Analogous results were obtained during ET_B-R stimulation in PKCβ1/CKAR expressing cells, confirming that receptor-dependent cPKC activation delimits the duration of its own receptor signal.

The question arises which cellular mechanisms account for the receptor-specific recruitment of PKCα and PKCβ. By comparing the Ca^{2+}-stoichiometry [47] and the Ca^{2+}-dependence of membrane binding of different PKC-C2 domains as a prerequisite of PKC activation [48], several studies came to the conclusion that PKCα is more sensitive to small changes of cytosolic $[Ca^{2+}]$ ($[Ca^{2+}]½ = 1.4$ μmol/L [47] than other cPKC isoforms. Therefore, during small $[Ca^{2+}]_i$ transients, PKCα is expected to dock more efficiently to the plasma membrane than PKCβ [48]. In contrast, the C2 domain of PKCβ is activated at higher $[Ca^{2+}]$ ($[Ca^{2+}]½ = 5$ μmol/L [47] but responds more efficiently to smaller fractional changes in $[Ca^{2+}]_i$ than PKCα. A recent study investigated the translocation of GFP*(green fluorescent protein)*-tagged cPKC isoforms to the membrane of HEK293 cells and described some interesting differences in the time courses of PKCα and PKCβ translocation/dissociation [49]. During stimulation of α_1-AR with Phe (100 μmol/L), both PKCα and PKCβ rapidly translocated to the cell membrane. In the continuous presence of Phe, PKCα gradually returned to the cytosol whereas PKCβ resides at the plasma membrane.

These differences in the spatio-temporal dynamics of cPKC isoform translocation might elucidate the mechanism of receptor-specific PKCα and PKCβ activation in the present study. Although the experimental tools used in the present study are not appropriate to quantify the intracellular Ca^{2+} concentration, we are confident that the novel Ca^{2+}-biosensor Twitch-2B with its high dynamic range [30] provides a reliable tool to monitor G_qPCR-induced increases in $[Ca^{2+}]_i$ with high temporal resolution. As shown in Fig. 9, the Twitch-2B sensor reported receptor-specific differences in the onset and amplitude of G_qPCR-induced $[Ca^{2+}]_i$ transients that might account for different temporal activation of PKCα and PKCβ. According to the high Ca^{2+} affinity of PKCα, the relatively small increase in $[Ca^{2+}]_i$ during stimulation of α_{1B}-ARs might be sufficient to activate PKCα whereas activation of PKCβ with its low Ca^{2+}-affinity requires a pronounced increase in $[Ca^{2+}]_i$ as observed during ET-receptor stimulation.

The receptor-specific activation of PKCα and PKCβ and the feedback modulation of G_qPCR activity investigated in the present study, may account for some differences in the G_qPCR-induced modulation of cardiac physiology. Activation of α_{1B}-receptors induces positive inotropic and chronotropic effects in mouse atrium [50] which is compatible with IP_3-induced Ca^{2+}-release and GIRK inhibition. Accordingly, the endothelin-1-mediated inhibition of $IK_{(ACh)}$, which is predominantly mediated by ET_A receptors, but also partially by ET_B-receptors, has been accounted for positive chronotropic effects of endothelin in rabbit atrial myocytes [51]. However, the extent of GIRK inhibition during α_{1B}-AR- and ET-R activation was significantly different in mouse atrial myocytes with moderate inhibitory effects of phenylephrine and pronounced GIRK inhibition by ET-1 [7]. These differences were attributed to receptor-dependent differences in local PIP_2-depletion that might account for receptor-specific GIRK inhibition [18].

We have evidence that the rapid α_{1B}-AR-desensitization delimits the duration of the receptor signal thus confining the activation of downstream G_q pathways. Pronounced GIRK inhibition during ET-receptor activation corresponds to the long-lasting ET-receptor activity and slow homologous receptor desensitization.

Apart from short-term inotropic effects of α_1-AR and ET-R stimulation, activation of both receptors has been shown to contribute to cardiac hypertrophy, cardiomyopathy and cardiac remodeling (for reviews see [52] and references therein, [53]). To the best of our knowledge there are no studies that investigate the specific contribution of α_{1B}-induced PKCα activation and ET-R-induced activation of PKCβ to cardiac pathophysiology. Since the activation profile of individual PKC isoenzymes during G_qPCR stimulation is receptor-dependent and varies among species ([54] and references therein), the contribution of specific PKC isoforms to the pathophysiology of heart failure and cardiac hypertrophy is discussed controversially. Several studies demonstrated a significant contribution of either PKCα [55] or PKCβ1 [56] to the pathogenesis of heart failure, others postulated a dominant role of PKCβII and PKCε activation (e.g [57] for review see [58]. Further conflicting results were reported for the activation of PKC isoforms in the human heart and its contribution to heart failure. Increased activity of PKCα, PKCβ1 and PKCβ2 was reported in left ventricles of human hearts [56], but specific activation of the (novel) nPKCs ε and δ during stimulation of endothelin and α-adrenergic receptors in human atria [54].

Although signalling specificity during G_qPCR-activation is required for the specialized functions of different PKC isoforms in sometimes divergent downstream signalling pathways, the specific contribution of α_{1B}-induced PKCα- and ET-R-induced PKCβ activation to cardiac pathophysiology remains to be elucidated.

5. Conclusions

Apart from PIP_2-depletion as the underlying mechanism of GIRK-inhibition in rat atrial myocytes upon activation of G_q-coupled receptors, we demonstrate a component of receptor-induced GIRK inhibition that is attributed to the activation of Ca^{2+}-dependent PKC isoforms (cPKC). Pharmacological block of specific cPKC isoforms significantly reduced receptor-species dependent GIRK inhibition, supporting the notion that receptor-specific activation of the cPKC isoforms PKCα (by α_1-ARs) and PKCβ (by ET-Rs) accounts for receptor-

dependent differences in GIRK inhibition. Furthermore, we attribute the different efficacies of α_1-AR and ET-R to induce GIRK inhibition to receptor-specific differences in homologous receptor desensitization that controls the duration and the specificity of PKC activation. The recruitment of different cPKC isoforms exerts a negative feedback on homologous receptor activity thus limiting the strength and duration of the receptor signal and as a consequence the efficiency of GIRK inhibition.

Funding

This research did not receive any specific grant from funding agencies in the public, commercial, or not-for-profit sector.

Authorship contribution

Participated in research design: M.-C. K.

Provided reagents and analytical tools: A. R.

Conducted experiments and performed data analysis: A. N., M.-C. K.

Wrote the manuscript or contributed to the manuscript.: M.-C. K., A. R.

All authors confirm that they have read and approved the final version of this manuscript.

Declaration of Competing Interest

The authors report no conflict of interest.

Acknowledgement

We thank Lutz Pott for helpful scientific discussions and Anke Galhoff and Bing Liu for expert technical assistance.

References

[1] H. Hibino, A. Inanobe, K. Furutani, S. Murakami, I. Findlay, Y. Kurachi, Inwardly rectifying potassium channels, Physiol. Rev. 90 (2010) 291–366.
[2] H. Cho, Regulation of adenosine-activated GIRK channels by Gq-coupled receptors in mouse atrial Myocytes, Korean J. Physiol. Pharmacol. Off. J. Korean Physiol. Soc. Korean Soc. Pharmacol. 14 (2010) 145–150.
[3] C. Müllner, D. Vorobiov, A.K. Bera, Y. Uezono, D. Yakubovich, B. Frohnwieser-Steinecker, N. Dascal, W. Schreibmayer, Heterologous facilitation of G protein-activated K^+ channels by beta-adrenergic stimulation via cAMP-dependent protein kinase, J. G. Physiol. 115 (2000) 547–558.
[4] J.J. Hill, E.G. Peralta, Inhibition of a G_i-activated potassium channel (GIRK1/4) by the G_q-coupled m_1 muscarinic acetylcholine receptor, J. Biol. Chem. 276 (2001) 5505–5510.
[5] T. Meyer, M.C. Wellner-Kienitz, A. Biewald, K. Bender, A. Eickel, L. Pott, Depletion of phosphatidylinositol 4,5-bisphosphate by activation of phospholipase C-coupled receptors causes slow inhibition but not desensitization of G protein-gated inward rectifier K^+ current in atrial myocytes, J. Biol. Chem. 276 (2001) 5650–5658.
[6] Q. Lei, M.B. Jones, E.M. Talley, J.C. Garrison, D.A. Bayliss, Molecular mechanisms mediating inhibition of G protein-coupled inwardly-rectifying K^+ channels, Mol. Cell 15 (2003) 1–9.
[7] H. Cho, D. Lee, S.H. Lee, W.-K. Ho, Receptor-induced depletion of phosphatidylinositol 4,5-bisphosphate inhibits inwardly rectifying K^+ channels in a receptor-specific manner, Proc. Natl. Acad. Sci. U. S. A. 102 (2005) 4643–4648.
[8] J.-W. Sohn, D. Lee, H. Cho, W. Lim, H.-S. Shin, S.-H. Lee, W.-K. Ho, Receptor-specific inhibition of $GABA_B$-activated K^+ currents by muscarinic and metabotropic glutamate receptors in immature rat hippocampus, J. Physiol. 580 (2007) 411–422.
[9] S. Cui, W.-K. Ho, S.-T. Kim, H. Cho, Agonist-induced localization of G_q-coupled receptors and G protein-gated inwardly rectifying K+ (GIRK) channels to caveolae determines receptor specificity of phosphatidylinositol 4,5-bisphosphate signaling, J. Biol. Chem. 285 (2010) 41732–41739.
[10] J.-W. Sohn, A. Lim, S.-H. Lee, W.-K. Ho, Decrease in PIP_2 channel interactions is the final common mechanism involved in PKC- and arachidonic acid-mediated inhibitions of $GABA_B$-activated K^+ current, J. Physiol. 582 (2007) 1037–1046.
[11] F. Hertel, A. Switalski, E. Mintert-Jancke, K. Karavassilidou, K. Bender, L. Pott, M.-C. Kienitz, A genetically encoded tool kit for manipulating and monitoring membrane phosphatidylinositol 4,5-bisphosphate in intact cells, PLoS One 6 (2011) e20855.
[12] M.R. Whorton, R. MacKinnon, Crystal structure of the mammalian GIRK2 K^+ channel and gating regulation by G proteins, PIP_2, and sodium, Cell 147 (2011) 199–208.
[13] J. Mao, X. Wang, F. Chen, R. Wang, A. Rojas, Y. Shi, H. Piao, C. Jiang, Molecular basis for the inhibition of G protein-coupled inward rectifier K^+ channels by protein kinase C, Proc. Natl. Acad. Sci. U. S. A. 101 (2004) 1087–1092.
[14] S.K. Adney, J. Ha, X.-Y. Meng, T. Kawano, D.E. Logothetis, A critical gating switch at a modulatory site in neuronal Kir3 channels, J. Neurosci. 35 (2015) 14397–14405.
[15] L. Zhang, J.-K. Lee, S.A. John, N. Uozumi, I. Kodama, Mechanosensitivity of GIRK channels is mediated by protein kinase C-dependent channel-phosphatidylinositol 4,5-bisphosphate interaction, J. Biol. Chem. 279 (2004) 7037–7047.
[16] I. Keselman, M. Fribourg, D.P. Felsenfeld, D.E. Logothetis, Mechanism of PLC-mediated Kir3 current inhibition, Channels (Austin) 1 (2007) 113–123.
[17] M.J. Berridge, Inositol trisphosphate and diacylglycerol, Annu. Rev. Biochem. 56 (1987) 159–193.
[18] H. Cho, Y.A. Kim, J.-Y. Yoon, D. Lee, J.H. Kim, S.H. Lee, W.-K. Ho, Low mobility of phosphatidylinositol 4,5-bisphosphate underlies receptor specificity of G_q-mediated ion channel regulation in atrial myocytes, Proc. Natl. Acad. Sci. U. S. A. 102 (2005) 15241–15246.
[19] J.L. Leaney, L.V. Dekker, A. Tinker, Regulation of a G protein-gated inwardly rectifying K^+ channel by a Ca^{2+}-independent protein kinase C, J. Physiol. 534 (2001) 367–379.
[20] S.G. Brown, A. Thomas, L.V. Dekker, A. Tinker, J.L. Leaney, PKC-delta sensitizes Kir3.1/3.2 channels to changes in membrane phospholipid levels after M_3 receptor activation in HEK-293 cells, Am. J. Physiol. Cell Physiol. 289 (2005) C543–C556.
[21] E.N. Nikolov, T.T. Ivanova-Nikolova, Coordination of membrane excitability through a GIRK1 signaling complex in the atria, J. Biol. Chem. 279 (2004) 23630–23636.
[22] R.K. Singh, S. Kumar, P.K. Gautam, M.S. Tomar, P.K. Verma, S.P. Singh, A. Acharya, Protein kinase C-α and the regulation of diverse cell responses, Biomol. Concepts 8 (2017) 143–153.
[23] K. Taguchi, M. Yang, M. Goepel, M.C. Michel, Comparison of human alpha1-adrenoceptor subtype coupling to protein kinase C activation and related signalling pathways, Naunyn Schmiedebergs Arch. Pharmacol. 357 (1998) 100–110.
[24] M.-C. Kienitz, D. Vladimirova, C. Müller, L. Pott, A. Rinne, Receptor species-dependent desensitization controls KCNQ1/KCNE1 K^+ channels as downstream effectors of G_q protein-coupled receptors, J. Biol. Chem. 291 (2016) 26410–26426.
[25] A. Policha, N. Daneshtalab, L. Chen, L.B. Dale, C. Altier, H. Khosravani, W.G. Thomas, G.W. Zamponi, S.S.G. Ferguson, Role of angiotensin II type 1A receptor phosphorylation, phospholipase D, and extracellular calcium in isoform-specific protein kinase C membrane translocation responses, J. Biol. Chem. 281 (2006) 26340–26349.
[26] L.L. Gallegos, A.C. Newton, Spatiotemporal dynamics of lipid signaling, IUBMB Life 60 (2008) 782–789.
[27] M. Hoque, C. Rentero, R. Cairns, F. Tebar, C. Enrich, T. Grewal, Annexins - scaffolds modulating PKC localization and signaling, Cell. Signal. 26 (2014) 1213–1225.
[28] J.D. Violin, J. Zhang, R.Y. Tsien, A.C. Newton, A genetically encoded fluorescent reporter reveals oscillatory phosphorylation by protein kinase C, J. Cell Biol. 161 (2003) 899–909.
[29] Y. Murata, H. Iwasaki, M. Sasaki, K. Inaba, Y. Okamura, Phosphoinositide phosphatase activity coupled to an intrinsic voltage sensor, Nature 435 (2005) 1239–1243.
[30] T. Thestrup, J. Litzlbauer, I. Bartholomaus, M. Mues, L. Russo, H. Dana, Y. Kovalchuk, Y. Liang, G. Kalamakis, Y. Laukat, S. Becker, G. Witte, A. Geiger, T. Allen, L.C. Rome, T.-W. Chen, D.S. Kim, O. Garaschuk, C. Griesinger, O. Griesbeck, Optimized ratiometric calcium sensors for functional in vivo imaging of neurons and T lymphocytes, Nat. Methods 11 (2014) 175–182.
[31] J.-W. Soh, I.B. Weinstein, Roles of specific isoforms of protein kinase C in the transcriptional control of cyclin D1 and related genes, J. Biol. Chem. 278 (2003) 34709–34716.
[32] K. Bender, M.-C. Wellner-Kienitz, L.I. Bosche, A. Rinne, C. Beckmann, L. Pott, Acute desensitization of GIRK current in rat atrial myocytes is related to K+ current flow, J. Physiol. 561 (2004) 471–483.
[33] K. Bender, M.-C. Wellner-Kienitz, L. Pott, Transfection of a phosphatidyl-4-phosphate 5-kinase gene into rat atrial myocytes removes inhibition of GIRK current by endothelin and alpha-adrenergic agonists, FEBS Lett. 529 (2002) 356–360.
[34] Y. Kurachi, H. Ito, T. Sugimoto, T. Shimizu, I. Miki, M. Ui, Alpha-adrenergic activation of the muscarinic K^+ channel is mediated by arachidonic acid metabolites, Pflugers Arch. Eur. J. Physiol. 414 (1989) 102–104.
[35] J.D. Violin, S.M. Dewire, W.G. Barnes, R.J. Lefkowitz, G protein-coupled receptor kinase and beta-arrestin-mediated desensitization of the angiotensin II type 1A receptor elucidated by diacylglycerol dynamics, J. Biol. Chem. 281 (2006) 36411–36419.
[36] H. Iwasaki, Y. Murata, Y. Kim, M.I. Hossain, C.A. Worby, J.E. Dixon, T. McCormack, T. Sasaki, Y. Okamura, A voltage-sensing phosphatase, Ci-VSP, which shares sequence identity with PTEN, dephosphorylates phosphatidylinositol 4,5-bisphosphate, Proc. Natl. Acad. Sci. U. S. A. 105 (2008) 7970–7975.
[37] S. Makary, N. Voigt, A. Maguy, R. Wakili, K. Nishida, M. Harada, D. Dobrev, S. Nattel, Differential protein kinase C isoform regulation and increased constitutive activity of acetylcholine-regulated potassium channels in atrial remodeling, Circ. Res. 109 (2011) 1031–1043.
[38] C.F. Lo, G.E. Breitwieser, Protein kinase-independent inhibition of muscarinic K+ channels by staurosporine, Am. J. Physiol. 266 (1994) C1128–C1132.
[39] K. Mubagwa, R. Macianskiene, S. Viappiani, V. Gendviliene, B. Carlsson, B. Brandts, KB130015, a new amiodarone derivative with multiple effects on cardiac ion channels, Cardiovasc. Drug Rev. 21 (2003) 216–235.
[40] B. Brandts, R. Borchard, R. Macianskiene, V. Gendviliene, D. Dirkmann, M. van Bracht, M. Prull, M. Meine, I. Wickenbrock, K. Mubagwa, H.-J. Trappe, Inhibition of G protein-coupled and ATP-sensitive potassium currents by 2-methyl-3-(3,5-diiodo-

4-carboxymethoxybenzyl)benzofuran (KB130015), an amiodarone derivative, J. Pharmacol. Exp. Ther. 308 (2004) 134–142.
[41] G. Martiny-Baron, M.G. Kazanietz, H. Mischak, P.M. Blumberg, G. Kochs, H. Hug, D. Marme, C. Schachtele, Selective inhibition of protein kinase C isozymes by the indolocarbazole go 6976, J. Biol. Chem. 268 (1993) 9194–9197.
[42] S.E. Wilkinson, P.J. Parker, J.S. Nixon, Isoenzyme specificity of bisindolylmaleimides, selective inhibitors of protein kinase C, Biochem. J. 294 (1993) 335–337 Pt 2.
[43] J.R. Graff, A.M. McNulty, K.R. Hanna, B.W. Konicek, R.L. Lynch, S.N. Bailey, C. Banks, A. Capen, R. Goode, J.E. Lewis, L. Sams, K.L. Huss, R.M. Campbell, P.W. Iversen, B.L. Neubauer, T.J. Brown, L. Musib, S. Geeganage, D. Thornton, The protein kinase Cbeta-selective inhibitor, Enzastaurin (LY317615.HCl), suppresses signaling through the AKT pathway, induces apoptosis, and suppresses growth of human colon cancer and glioblastoma xenografts, Cancer Res. 65 (2005) 7462–7469.
[44] W.J. van Blitterswijk, B. Houssa, Properties and functions of diacylglycerol kinases, Cell. Signal. 12 (2000) 595–605.
[45] B.H. Falkenburger, E.J. Dickson, B. Hille, Quantitative properties and receptor reserve of the DAG and PKC branch of G_q-coupled receptor signaling, J. G. Physiol. 141 (2013) 537–555.
[46] T. Kajimoto, S. Sawamura, Y. Tohyama, Y. Mori, A.C. Newton, Protein kinase C {delta}-specific activity reporter reveals agonist-evoked nuclear activity controlled by Src family of kinases, J. Biol. Chem. 285 (2010) 41896–41910.
[47] S.C. Kohout, S. Corbalan-Garcia, A. Torrecillas, J.C. Gomez-Fernandez, J.J. Falke, C2 domains of protein kinase C isoforms alpha, beta, and gamma, Biochemistry 41 (2002) 11411–11424.
[48] M. Guerrero-Valero, C. Marin-Vicente, J.C. Gomez-Fernandez, S. Corbalan-Garcia, The C2 domains of classical PKCs are specific PtdIns(4,5)P_2-sensing domains with different affinities for membrane binding, J. Mol. Biol. 371 (2007) 608–621.
[49] J. O-Uchi, J. Sorenson, B.S. Jhun, J. Mishra, S. Hurst, K. Williams, S.-S. Sheu, C.M.B. Lopes, Isoform-specific dynamic translocation of PKC by alpha1-adrenoceptor stimulation in live cells, Biochem. Biophys. Res. Commun. 465 (2015) 464–470.
[50] S. Zhang, R. Takahashi, N. Yamashita, H. Teraoka, T. Kitazawa, Alphalpha1B-adrenoceptor-mediated positive inotropic and positive chronotropic actions in the mouse atrium, Eur. J. Pharmacol. 839 (2018) 82–88.
[51] J.P. Spiers, E.J. Kelso, B.J. McDermott, C.N. Scholfield, B. Silke, Endothelin-1 mediated inhibition of the acetylcholine-activated potassium current from rabbit isolated atrial cardiomyocytes, Br. J. Pharmacol. 119 (1996) 1427–1437.
[52] A.J. Baker, Adrenergic signaling in heart failure, Pflugers Arch. Eur. J. Physiol. 466 (2014) 1139–1150.
[53] T. Miyauchi, S. Sakai, Endothelin and the heart in health and diseases, Peptides 111 (2019) 77–88.
[54] J.D. Kilts, H.P. Grocott, M.M. Kwatra, G alpha(q)-coupled receptors in human atrium function through protein kinase C epsilon and delta, J. Mol. Cell. Cardiol. 38 (2005) 267–276.
[55] J.C. Braz, K. Gregory, A. Pathak, W. Zhao, B. Sahin, R. Klevitsky, T.F. Kimball, J.N. Lorenz, A.C. Nairn, S.B. Liggett, I. Bodi, S. Wang, A. Schwartz, E.G. Lakatta, A.A. DePaoli-Roach, J. Robbins, T.E. Hewett, J.A. Bibb, M.V. Westfall, E.G. Kranias, J.D. Molkentin, PKC-alpha regulates cardiac contractility and propensity toward heart failure, Nat. Med. 10 (2004) 248–254.
[56] N. Bowling, R.A. Walsh, G. Song, T. Estridge, G.E. Sandusky, R.L. Fouts, K. Mintze, T. Pickard, R. Roden, M.R. Bristow, H.N. Sabbah, J.L. Mizrahi, G. Gromo, G.L. King, C.J. Vlahos, Increased protein kinase C activity and expression of Ca2 + −sensitive isoforms in the failing human heart, Circulation 99 (1999) 384–391.
[57] J.C.B. Ferreira, J.C. Campos, N. Qvit, X. Qi, L.H.M. Bozi, L.R.G. Bechara, V.M. Lima, B.B. Queliconi, M.-H. Disatnik, P.M.M. Dourado, A.J. Kowaltowski, D. Mochly-Rosen, A selective inhibitor of mitofusin 1-βIIPKC association improves heart failure outcome in rats, Nat. Commun. 10 (2019) 329.
[58] J.C.B. Ferreira, P.C. Brum, D. Mochly-Rosen, βIIPKC and εPKC isozymes as potential pharmacological targets in cardiac hypertrophy and heart failure, J. Mol. Cell. Cardiol. 51 (2011) 479–484.